Group-Blind Detection for Uplink of Massive MIMO Systems

Guido Carlo Ferrante, *Member, IEEE,* Giovanni Geraci, *Member, IEEE,* Tony Q. S. Quek, *Senior Member, IEEE,* and Moe Z. Win, *Fellow, IEEE*

***Abstract*—When paired with traditional channel estimation and detection, massive MIMO is severely affected by pilot contamination. While sticking to the traditional structure of the training phase, where orthogonal pilot sequences are reused in different cells, we propose a group-blind detector that takes into account the presence of pilot contamination. Our detector uses the excess antennas to partially remove interference during the data transmission phase. We derive asymptotic expressions for the SINR gain and the achievable rate in the massive regime, i.e., when the number of antennas tends to infinity while keeping the number of users per cell fixed. Implementing the group-blind detector requires an estimate of the aggregate out-of-cell channel covariance. We propose a simple scheme, referred to as *method of silences*, to obtain such estimate. Numerical results confirm our analysis in practical scenarios, and show cases where the *method of silences* achieves a large fraction of the promised SINR gain over conventional detectors.**

***Index Terms*—Multiuser MIMO, group-blind detection, large antenna arrays, pilot contamination, interference suppression.**

I. Introduction

MASSIVE MIMO and cell densification are two technologies promising to boost the rate per unit area in future (5G) cellular networks: in the former, the number of antennas at each base station (BS) is increased; in the latter, the number of BSs is increased [2]–[5]. In both cases, interference may limit the achievable rate as the total number of antennas grows [6]–[10]. In massive MIMO, the rate is bounded by the inability of the BS to acquire accurate channel estimation during the training phase [11]–[13]. This is due to the fact that the number of orthogonal pilots available for training is limited by the coherence time of the channel: for typical values of the coherence time, it is not possible to allocate orthogonal pilots to all users in the network but just to users within each cell. Therefore, the same set of pilots has to be reused in different cells, which causes a channel estimation impairment known as *pilot contamination* [11]. In this article, we design a detector for the uplink of massive MIMO that reduces the detrimental effect of pilot contamination to increase the transmission rate.

A. Background and Motivation

In massive MIMO, a multitude of small and individually controlled antennas performs multiplexing and demultiplexing for all active users. Adding more antennas helps to reduce radiated power, simplify the signal processing operations, and meet the ever-increasing wireless data demand [14]–[16]. In fact, under accurate channel state information (CSI), fifty-fold or greater spectral efficiency improvements are envisioned over the current (4G) technology [17]–[20]. However, in practice, the training phase of large-scale antenna systems suffers from pilot contamination, which may in turn jeopardize the achievable rate during the data transmission phase [21], [22]. This is the case, in particular, when traditional receivers are used as though the CSI were perfect [23]–[27], which incurs in a possible rate loss. It is of critical importance to compensate for the incurred loss. Such compensation can be partly achieved by exploiting the excess dimensions in the signal space that are made available by the presence of a large number of antennas. The effect of imperfect channel estimation on wireless systems employing multiple antennas is characterized in [28]–[35].

In order to mitigate pilot contamination through a modified channel estimation phase, a non-linear iterative algorithm that jointly estimates channels and transmitted symbols was proposed in [36], obtaining an improvement in terms of symbol error probability with respect to linear algorithms. A step towards understanding the fundamental limits of massive MIMO was recently made in [37]–[39], showing that pilot contamination can be removed if the power received from in-cell users is larger than the one received from out-of-cell users. However, this assumption requires both power control and a regular cell geometry, and it may not hold in full generality [40]. The irregular topology of current cellular networks calls for new multiuser detectors to mitigate the effect of pilot contamination.

In this paper, we focus on the uplink rate of massive MIMO systems. We propose a detector that takes into account pilot contamination. The uplink is a limiting factor in mobile networks, in particular because of the poor link budget [41], [42]. The problem is exacerbated with the ever increasing traffic from terminals to base stations, especially driven by

Manuscript received December 1, 2015; revised August 5, 2016; accepted October 4, 2016. The associate editor coordinating the review was Prof. J. Jaldén. This paper was presented in part at the 2016 IEEE Int. Conf. Acoust. Speech Signal Process. (ICASSP), Shanghai, China [1].

Guido Carlo Ferrante is with the Information Systems Technology and Design (ISTD) Pillar, Singapore University of Technology and Design, 487372 Singapore, and with the Laboratory for Information and Decision Systems (LIDS), Massachusetts Institute of Technology, Cambridge, MA 02139 USA (e-mail: gcf@ieee.org; gcfer@mit.edu).

Giovanni Geraci was with Singapore University of Technology and Design, 487372 Singapore. He is now with Nokia Bell Labs, Dublin D15 Y6NT Ireland (e-mail: giovanni.geraci@nokia.com).

Tony Q. S. Quek is with the Information Systems Technology and Design Pillar, Singapore University of Technology and Design, 487372 Singapore (e-mail: tonyquek@sutd.edu.sg).

Moe Z. Win is with the Laboratory for Information and Decision Systems (LIDS), Massachusetts Institute of Technology, Cambridge, MA 02139 USA (e-mail: moewin@mit.edu).

cloud storage and social networking applications as well as the number of connected devices [43], [44]. Therefore, uplink improvements were pursued during the evolution of LTE [45]. Novel design and performance analysis for the uplink have been receiving considerable attention in the last few years [22], [46]–[50]. The proposed detector is compatible with existing downlink schemes as well as different receiver designs that aim at providing better channel estimations. Our detector tries to reduce the effect of imperfect estimation due to contamination once the latter is present.

B. Approach and Contributions

In this paper, we design and analyze a group-blind detector for the uplink of massive MIMO in the presence of pilot contamination. The proposed design does not require power control or regular cell tessellation. It generalizes group-blind detection, introduced in the context of CDMA [51]–[54], to the case of imperfect channel knowledge. For the practical implementation of the group-blind detector, we propose a modified structure of the data transmission phase based on blanking. In particular, the blanking technique provides a method to estimate a second-order channel statistics needed to implement the detector without requiring any cooperation among cells. In this paper, we develop a framework that allows to use group-blind detection in the uplink of cellular networks affected by pilot contamination, and derive a group-blind detector that is shown to maximize the SINR at the BS within a class of group-blind detectors. We discuss also implementation issues, and present analytical and numerical results of interest in practical scenarios. Our main contributions are summarized as follows.

- We derive a group-blind detector that accounts for imperfect channel knowledge of in-cell users, which is motivated by the presence of contamination in the uplink of massive MIMO. The group-blind detector can be regarded as a generalization of traditional detectors, such as matched filter (MF), MMSE, and regularized zero forcing (RZF), which use the contaminated channel knowledge as though it were perfect. Our approach exploits excess dimensions in the signal space that are made available by the presence of excess antennas, and partially regains the loss due to general channel estimation impairments.
- We analyze asymptotic SINR gains achievable by the group-blind detector with respect to traditional detectors when contamination is due to the use of orthogonal pilot sequences in different cells during the training phase. We find that the group-blind detector provides an SINR gain larger than unity even in a worst case propagation scenario. Numerical results validate our analytical derivations by exhibiting fast convergence towards asymptotic limits, and show that the gain achieved by the proposed detector is significant in scenarios of practical interest.
- We propose a practical implementation of the detector, which requires an estimate of the aggregate out-of-cell channel covariance. To obtain such estimate, we suggest a simple scheme, referred to as *method of silences*, based on a blanking technique that resembles the Almost Blank Subframes feature of LTE R12 [55]. In our scheme, users within each cell remain silent for a small subset of data symbols, pseudo-randomly and independently selected by each BS, thus allowing all BSs to estimate the aggregate instantaneous out-of-cell channel covariance.
- We evaluate the performance of the proposed group-blind detector when it is implemented jointly with the *method of silences*. Numerical results show that in some practical scenarios, the simple *method of silences* is sufficient to achieve a large fraction of the promised SINR gain, and a net ergodic rate significantly higher than that achieved by conventional receivers.

The rest of the paper is organized as follows. The system model is presented in Section II. Section III contains the derivation of the group-blind detector, and Section IV discusses implementation details. Section V presents asymptotic analytical results, while numerical results are provided in Section VI. The paper is concluded in Section VII.

C. Notations

Throughout the paper, n, K, and L stand for the number of antennas at each BS, the number of users in each cell, and the number of cells in the network, respectively. The massive regime corresponds to $n \to \infty$ while keeping K and L finite. Given two sequences $(\mathsf{x}_n)_{n\geqslant 0}$ and $(\mathsf{y}_n)_{n\geqslant 0}$ of random variables (RVs), almost sure (a.s.) convergence of x_n to y_n is denoted $\mathsf{x}_n \xrightarrow{\text{a.s.}} \mathsf{y}_n$. Asymptotic equivalence of two sequences, denoted $\mathsf{x}_n \asymp \mathsf{y}_n$, is defined by $\mathsf{x}_n - \mathsf{y}_n \xrightarrow{\text{a.s.}} 0$. We denote δ_{ij} the Kronecker symbol ($\delta_{ij} = 1$ if $i = j$, and $\delta_{ij} = 0$ otherwise), and $\mathbb{1}_P$ the indicator function of the statement P ($\mathbb{1}_P = 1$ when P is true, and $\mathbb{1}_P = 0$ otherwise). Random variables are displayed in sans serif, upright fonts; their realizations in serif, italic fonts. Vectors and matrices are denoted by bold lowercase and uppercase letters, respectively. For example, a random variable and its realization are denoted by x and x; a random vector and its realization are denoted by $\boldsymbol{\mathsf{x}}$ and $\boldsymbol{x}$; a random matrix and its realization are denoted by $\boldsymbol{\mathsf{X}}$ and $\boldsymbol{X}$; a random set is denoted by X. Direct sum of subspaces is denoted by $\oplus$. Given a vector $\boldsymbol{v}$, the transpose and hermitian transpose are denoted by $\boldsymbol{v}^\mathsf{T}$ and $\boldsymbol{v}^\dagger$, respectively. We denote $\mathrm{diag}(a_1, \ldots, a_n)$ the diagonal matrix with elements on the main diagonal equal to $a_1, \ldots, a_n$. The subspace spanned by set of vectors $\{\boldsymbol{v}_1, \ldots, \boldsymbol{v}_n\}$ is denoted by $\mathrm{range}\{\boldsymbol{v}_1, \ldots, \boldsymbol{v}_n\}$. With a slight abuse of notation, we denote $\mathrm{range}\{\boldsymbol{A}\}$ the subspace spanned by the columns of matrix $\boldsymbol{A}$, and $\mathrm{range}\{\boldsymbol{A}_1, \boldsymbol{A}_2, \ldots, \boldsymbol{A}_n\}$ the subspace spanned by the columns of matrix $[\boldsymbol{A}_1\ \boldsymbol{A}_2\ \cdots\ \boldsymbol{A}_n]$.

II. System Model

A. Received Signal

Consider the uplink of a noncooperative multicellular network with L cells sharing the same time-frequency resource blocks. Each cell is equipped with one BS having n antennas. For the sake of simplicity, we assume that each cell includes K single-antenna users. Throughout the paper, the reference cell is referred to as cell 1, and interfering cells are labeled with indices $l \in \{2, 3, \ldots, L\}$. Users in the reference cell and

$$\gamma_{1k} = \frac{|\mathbf{w}_{1k}^\dagger \hat{\mathbf{g}}_{1k}|^2}{\mathbb{E}\left\{ \mathbf{w}_{1k}^\dagger \left(\frac{1}{P}\boldsymbol{I} + \tilde{\mathbf{g}}_{1k}\tilde{\mathbf{g}}_{1k}^\dagger + \sum_{j\neq k} \mathbf{g}_{1j}\mathbf{g}_{1j}^\dagger + \sum_{l>1}\sum_{j\geqslant 1} \mathbf{g}_{lj}\mathbf{g}_{lj}^\dagger \right) \mathbf{w}_{1k} \,\middle|\, \hat{\mathbf{G}}_1 \right\}}. \tag{10}$$

in other cells will be referred to as *in-cell users* and *out-of-cell users*, respectively. The signal received by the BS of the reference cell (reference BS) during symbol period m is:

$$\mathbf{y}(m) = \sum_{l=1}^{L}\sum_{k=1}^{K} \mathbf{h}_{lk}\sqrt{\beta_{lk}}\,\mathsf{x}_{lk}(m) + \mathbf{n}(m), \tag{1}$$

where: $\mathbf{y}(m) \in \mathbb{C}^n$; $\mathbf{h}_{lk} = [\mathsf{h}_{lk1}, \mathsf{h}_{lk2}, \ldots, \mathsf{h}_{lkn}]^\mathsf{T} \in \mathbb{C}^n$ is the channel vector between user k in cell l and the BS of the reference cell, with h_{lkr} being the channel coefficient with respect to BS antenna r; $\beta_{lk} > 0$ captures the effect of pathloss and shadowing for user k in cell l, and is assumed constant within each coherence time; $\mathsf{x}_{lk}(m)$ is the symbol transmitted by user k in cell l; $\mathbf{n}(m) \in \mathbb{C}^n$ is the additive white Gaussian noise (AWGN) vector. We assume $\mathsf{h}_{lkr} \sim \mathcal{CN}(0,1)$, and:

$$\mathbb{E}\{\, \mathbf{n}(m)\mathbf{n}(m')^\dagger \,\} = \boldsymbol{I}\delta_{mm'}, \tag{2}$$

$$\mathbb{E}\{\, \mathbf{h}_{lk}\mathbf{h}_{l'k'}^\dagger \,\} = \boldsymbol{I}\delta_{ll'}\delta_{kk'}, \tag{3}$$

$$\mathbb{E}\{\, \mathsf{x}_{lk}(m)\mathsf{x}_{l'k'}(m')^* \,\} = P\delta_{ll'}\delta_{kk'}\delta_{mm'}, \tag{4}$$

where P is the transmitted power, which is the same for all users. Note that model (1) can capture different reuse factors by choosing appropriate values of β_{lk} and L. Denoting $\mathbf{H}_l := [\mathbf{h}_{l1}, \mathbf{h}_{l2}, \ldots, \mathbf{h}_{lK}] \in \mathbb{C}^{n\times K}$, $\boldsymbol{R}_l := \mathrm{diag}(\beta_{l1}, \beta_{l2}, \ldots, \beta_{lK})$, $\mathbf{G}_l := \mathbf{H}_l\boldsymbol{R}_l^{1/2}$, and $\mathbf{x}_l(m) = [\mathsf{x}_{l1}(m), \mathsf{x}_{l2}(m), \ldots, \mathsf{x}_{lK}(m)]^\mathsf{T} \in \mathbb{C}^{K\times 1}$ yields:

$$\mathbf{y} = \sum_{l=1}^{L} \mathbf{H}_l\boldsymbol{R}_l^{1/2}\mathbf{x}_l + \mathbf{n} = \sum_{l=1}^{L} \mathbf{G}_l\mathbf{x}_l + \mathbf{n}, \tag{5}$$

where dependence on the symbol period m is made implicit.

B. Channel Estimation

We consider channel estimation based on orthogonal training sequences (pilots) reused in each interfering cell [11], [22], [27]. Users within each cell are assigned to different training sequences drawn from a set of K orthogonal sequences. Note that the proposed detector can be used for any number of users that interfere during the training phase. We refer the reader to [11, Section VII-F] and [22] for a discussion on different pilots design, where it is shown that using non-orthogonal pilot sequences does not make a significant difference in terms of performance. Therefore, any in-cell user is interfered by one user per interfering cell. Denote T_d and T the length of data transmission phase and coherence time (expressed in symbol periods), respectively. The length of the training sequences is, therefore, $T_\tau = T - T_\mathsf{d}$ symbol periods with $T_\tau \geqslant K$ due to the assumed orthogonality of pilot sequences [12], [56]. The orthogonality of pilots also implies that the MMSE estimate $\hat{\mathbf{g}}_{1k}$ of $\mathbf{g}_{1k}$ at the BS is [25], [56], [57]:

$$\hat{\mathbf{g}}_{1k} = \left(\sum_{l\geqslant 1} \mathbf{g}_{lk} + \sqrt{\epsilon}\boldsymbol{\nu}_{1k} \right)\theta_{1k}, \tag{6}$$

where $\boldsymbol{\nu}_{1k} \sim \mathcal{CN}(\mathbf{0}, \boldsymbol{I})$, $\theta_{1k} = \varphi_{1k}\beta_{1k}^{-1}$ with

$$\varphi_{1k} = \frac{\beta_{1k}^2}{\epsilon + \sum_{l\geqslant 1}\beta_{lk}}, \tag{7}$$

and ϵ^{-1} is the effective training signal-to-noise ratio (SNR).

An important consequence of MMSE detection is that the estimation error $\tilde{\mathbf{g}}_{1k} = \mathbf{g}_{1k} - \hat{\mathbf{g}}_{1k}$ is uncorrelated with $\hat{\mathbf{g}}_{1k}$, due to the orthogonality principle: $\mathbb{E}\{\, \tilde{\mathbf{g}}_{1k}\hat{\mathbf{g}}_{1k}^\dagger \,\} = \mathbf{0}$ [11], [25]. Hence it results $\hat{\mathbf{g}}_{1k} \sim \mathcal{CN}(\mathbf{0}, \varphi_{1k}\boldsymbol{I})$ and $\tilde{\mathbf{g}}_{1k} \sim \mathcal{CN}(\mathbf{0}, (\beta_{1k} - \varphi_{1k})\boldsymbol{I})$.

C. Achievable Rate

The performance measure of interest in this paper is the rate achieved by the generic in-cell user, given the channel estimation acquired in the training phase [11], [25], [27]. Denoting the estimated channel by $\hat{\mathbf{G}}_1 = [\hat{\mathbf{g}}_{11}, \hat{\mathbf{g}}_{12}, \ldots, \hat{\mathbf{g}}_{1L}]$ and the estimation error by $\tilde{\mathbf{G}}_1 = [\tilde{\mathbf{g}}_{11}, \tilde{\mathbf{g}}_{12}, \ldots, \tilde{\mathbf{g}}_{1L}]$ allows rewriting (5) as follows:

$$\mathbf{y} = \hat{\mathbf{G}}_1\mathbf{x}_1 + \tilde{\mathbf{G}}_1\mathbf{x}_1 + \sum_{l>1} \mathbf{G}_l\mathbf{x}_l + \mathbf{n}. \tag{8}$$

Let $\mathbf{w}_{1k}$ denote the linear receiver for user k. An *achievable rate* is [25], [56]:

$$R_{1k} = \mathbb{E}\{\, \log(1+\gamma_{1k}) \,\} \tag{9}$$

where the expectation is with respect to estimated channels $\hat{\mathbf{G}}_1$, and the SINR γ_{1k} is given in (10) at the top of the page. Note that (9) is a *lower bound* on capacity and does not provide an ultimate performance of the system. For the purpose of deriving the group-blind detector, define the following quantity:

$$\mathbf{y}' = \hat{\mathbf{G}}_1\mathbf{x}_1 + \tilde{\mathbf{G}}_1\tilde{\mathbf{x}}_1 + \sum_{l>1} \mathbf{G}_l\mathbf{x}_l + \mathbf{n}, \tag{11}$$

where $\tilde{\mathbf{x}}_1$ is independent of any other variable and has same covariance as $\mathbf{x}_1$. As such, $\mathbf{y}'$ has SINR equal to (10), hence any SINR-based performance of the group-blind detector can be equivalently evaluated on $\mathbf{y}'$. Hereinafter, we denote $\mathsf{G} = \{\mathbf{G}_l\}_{l=1}^L$ and $\mathsf{G}' = \{\hat{\mathbf{G}}_1, \tilde{\mathbf{G}}_1\} \cup \{\mathbf{G}_l\}_{l=2}^L$.

Remark 1. Note that the column vectors in G are conditionally dependent given $\tilde{\mathbf{G}}_1$, and follow a multivariate Gaussian distribution whose conditional mean and covariance can be derived according to [58, Proposition 3.13]. Such conditional dependence will be taken into account in all numerical results provided in Section VI.

III. Group-Blind Detector

Blind detection was developed for equalization [59] and interference suppression in multiuser communications [60], and then generalized to group-blind detection [51] in the context of CDMA. In CDMA, blind techniques allow the receiver to detect the useful signal by knowing the signature sequence of the user to decode only. Group-blind techniques extend blind detection to the case where the receiver knows the signature sequence of a subset of users, rather than one user only. In the uplink of a cellular network, this corresponds to a BS knowing in-cell channels and being unaware of out-of-cell channels. The shortcoming of the application of group-blind techniques in the cellular networks framework is that the BS has an imperfect knowledge of in-cell channels, due to the presence of pilot contamination, rather than a perfect one, as assumed in traditional blind and group-blind detection techniques. In this section, we start by presenting in Section III-A the derivation of a group-blind detector in the case of perfect knowledge of in-cell channels by following [51], and then propose in Section III-B a group-blind detector that takes into account the imperfect (i.e., contaminated) channel knowledge of a subset of users.

A. Group-Blind Detection without Contamination

First consider a system without estimation errors, where the receiver has perfect knowledge of the in-cell channels $\mathbf{G}_1$, but has no knowledge about $\{\mathbf{G}_l\}_{l>1}$. The design of the group-blind detector is based on the decomposition of the signal space, $\mathrm{range}\{\mathbf{G}_1, \mathbf{G}_2, \dots, \mathbf{G}_L\}$, into the subspace spanned by in-cell channels, $\mathrm{range}\{\mathbf{G}_1\}$, and its orthogonal complement, $\mathrm{range}\{\breve{\mathbf{U}}_{\mathbf{G}_1}\}$:

$$\mathrm{range}\{\mathbf{G}_1, \mathbf{G}_2, \dots, \mathbf{G}_L\} = \mathrm{range}\{\mathbf{G}_1\} \oplus \mathrm{range}\{\breve{\mathbf{U}}_{\mathbf{G}_1}\}. \quad (12)$$

The columns of $\breve{\mathbf{U}}_{\mathbf{G}_1}$ in (12) span the subspace orthogonal to the columns of $\mathbf{G}_1$ within the signal space. Without loss of generality, the detector $\mathbf{w}_{1k}$ lying in the signal space can be decomposed as follows:

$$\begin{aligned} &\mathbf{w}_{1k} = \dot{\mathbf{w}}_{1k} + \breve{\mathbf{w}}_{1k}, \\ &\dot{\mathbf{w}}_{1k} \in \mathrm{range}\{\mathbf{G}_1\}, \\ &\breve{\mathbf{w}}_{1k} \in \mathrm{range}\{\breve{\mathbf{U}}_{\mathbf{G}_1}\}. \end{aligned} \quad (13)$$

There are two steps in the derivation of a group-blind receiver $\mathbf{w}_{1k}$ for user k. The first step consists of defining a (virtual) received signal comprising in-cell channels only,

$$\mathbf{y}_{\mathrm{in}} = \mathbf{G}_1 \mathbf{x}_1 + \mathbf{n} \quad (14)$$

and then deriving the receiver $\dot{\mathbf{w}}_{1k}$ in order to estimate x_{1k} from $\mathbf{y}_{\mathrm{in}}$ knowing $\mathbf{G}_1$. According to the MMSE criterion, one has

$$\dot{\mathbf{w}}_{1k} = \underset{\bar{\boldsymbol{w}}_{1k}}{\mathrm{argmin}}\, \mathbb{E}\{\, |\mathrm{x}_{1k} - \bar{\boldsymbol{w}}_{1k}^\dagger \mathbf{y}_{\mathrm{in}}|^2 \,\}. \quad (15)$$

The second step consists in deriving $\breve{\mathbf{w}}_{1k}$ to deal with the whole received signal; again, according to the MMSE criterion, one has

$$\breve{\mathbf{w}}_{1k} = \underset{\bar{\boldsymbol{w}}_{1k}}{\mathrm{argmin}}\, \mathbb{E}\{\, |\mathrm{x}_{1k} - (\dot{\mathbf{w}}_{1k} + \bar{\boldsymbol{w}}_{1k})^\dagger \mathbf{y}|^2 \,\} \quad (16)$$

with $\bar{\boldsymbol{w}}_{1k} \in \mathrm{range}\{\breve{\mathbf{U}}_{\mathbf{G}_1}\}$.

In practice, the signal space can be inferred without knowing all channels, by means of the spectral decomposition of the received signal covariance $\boldsymbol{C}_{\mathbf{y}|\mathsf{G}} = \mathbb{E}\{\, \mathbf{y}\mathbf{y}^\dagger \,|\, \mathsf{G} \,\}$,

$$\boldsymbol{C}_{\mathbf{y}|\mathsf{G}} = P\mathbf{G}_1\mathbf{G}_1^\dagger + P\sum_{l>1} \mathbf{G}_l\mathbf{G}_l^\dagger + \boldsymbol{I}. \quad (17)$$

Moreover, $\breve{\mathbf{U}}_{\mathbf{G}_1}$ in (12) can be found via the spectral decomposition of the subspace orthogonal to the in-cell subspace:

$$\boldsymbol{\Pi}_{\mathbf{G}_1}^\perp \boldsymbol{C}_{\mathbf{y}|\mathsf{G}} \boldsymbol{\Pi}_{\mathbf{G}_1}^\perp = \breve{\mathbf{U}}_{\mathbf{G}_1} \breve{\boldsymbol{\Lambda}}_{\mathbf{G}_1} \breve{\mathbf{U}}_{\mathbf{G}_1}^\dagger + \breve{\mathbf{U}}_{\mathbf{N}} \breve{\mathbf{U}}_{\mathbf{N}}^\dagger, \quad (18)$$

where $\boldsymbol{\Pi}_{\mathbf{G}_1}^\perp$ is the projector onto the subspace orthogonal to $\mathrm{range}\{\mathbf{G}_1\}$, given by

$$\boldsymbol{\Pi}_{\mathbf{G}_1}^\perp = \boldsymbol{I} - \boldsymbol{\Pi}_{\mathbf{G}_1} = \boldsymbol{I} - \mathbf{G}_1(\mathbf{G}_1^\dagger \mathbf{G}_1)^{-1}\mathbf{G}_1^\dagger, \quad (19)$$

and the columns of $\breve{\mathbf{U}}_{\mathbf{N}}$ span the noise subspace.

B. Group-Blind Detection in the Presence of Contamination

We now derive a group-blind detector in the presence of imperfect in-cell channel knowledge. Differently from the previous derivation, we now assume that the receiver no longer knows the exact channel $\mathbf{G}_1$, and it does not know the in-cell signal space either. Based on the knowledge of $\mathrm{range}\{\hat{\mathbf{G}}_1\}$, the signal space can be decomposed as follows:

$$\mathrm{range}\{\mathbf{G}_1, \mathbf{G}_2, \dots, \mathbf{G}_L\} = \mathrm{range}\{\hat{\mathbf{G}}_1\} \oplus \mathrm{range}\{\breve{\mathbf{U}}_{\hat{\mathbf{G}}_1}\}. \quad (20)$$

The columns of $\breve{\mathbf{U}}_{\hat{\mathbf{G}}_1}$ in (20) span the subspace orthogonal to the column of $\hat{\mathbf{G}}_1$ within the signal space. Note that the above decomposition is consistent with the SINR expression in (10). Without loss of generality, detector $\mathbf{w}_{1k} \in \mathrm{range}\{\mathbf{G}_1, \cdots, \mathbf{G}_L\}$ can be decomposed as follows:

$$\begin{aligned} &\mathbf{w}_{1k} = \dot{\mathbf{w}}_{1k} + \breve{\mathbf{w}}_{1k}, \\ &\dot{\mathbf{w}}_{1k} \in \mathrm{range}\{\hat{\mathbf{G}}_1\}, \\ &\breve{\mathbf{w}}_{1k} \in \mathrm{range}\{\breve{\mathbf{U}}_{\hat{\mathbf{G}}_1}\}. \end{aligned} \quad (21)$$

The detector design consists of two steps. In the first step, we consider the (virtual) received signal similar to (14):

$$\mathbf{y}_{\mathrm{in}} = \hat{\mathbf{G}}_1 \mathbf{x}_1 + \mathbf{n}. \quad (22)$$

As above, $\dot{\mathbf{w}}_{1k}$ is derived according to the MMSE criterion (cf. (15)), with $\mathbf{y}_{\mathrm{in}}$ given by (22). Explicitly,

$$\dot{\mathbf{w}}_{1k} = (\hat{\mathbf{G}}_1\hat{\mathbf{G}}_1^\dagger + \tfrac{1}{P}\boldsymbol{I})^{-1}\hat{\mathbf{g}}_{1k}. \quad (23)$$

In the second step, $\breve{\mathbf{w}}_{1k}$ is derived by taking into account the whole received signal. As above, $\breve{\mathbf{w}}_{1k}$ is derived according to the MMSE criterion (cf. (16)):

$$\breve{\mathbf{w}}_{1k} = \underset{\bar{\boldsymbol{w}}_{1k}}{\mathrm{argmin}}\, \mathbb{E}\{\, |\mathrm{x}_{1k} - (\dot{\mathbf{w}}_{1k} + \bar{\boldsymbol{w}}_{1k})^\dagger \mathbf{y}'|^2 \,\} \quad (24)$$

with $\bar{\boldsymbol{w}}_{1k} \in \mathrm{range}\{\breve{\mathbf{U}}_{\hat{\mathbf{G}}_1}\}$. Following a derivation similar to that in [51, eq. (60)] and using the orthogonality between $\breve{\mathbf{U}}_{\hat{\mathbf{G}}_1}$ and $\hat{\mathbf{G}}_1$ yields:

$$\breve{\mathbf{w}}_{1k} = -\breve{\mathbf{U}}_{\hat{\mathbf{G}}_1}\Big(\breve{\mathbf{U}}_{\hat{\mathbf{G}}_1}^\dagger \boldsymbol{C}_{\mathbf{y}|\mathsf{G}} \breve{\mathbf{U}}_{\hat{\mathbf{G}}_1}\Big)^{-1} \breve{\mathbf{U}}_{\hat{\mathbf{G}}_1}^\dagger \boldsymbol{C}_{\mathbf{y}'|\mathsf{G}'} \dot{\mathbf{w}}_{1k}, \quad (25)$$

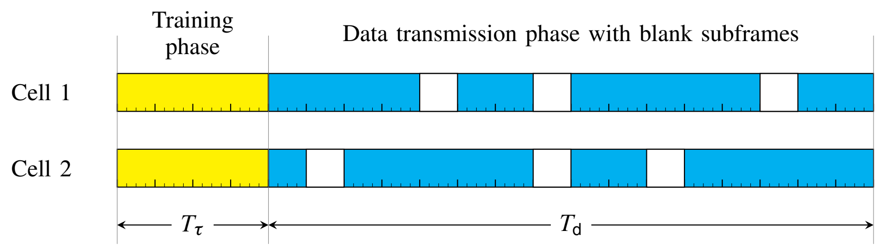

FIG. 1: Frame structure for generic users in Cell 1 and Cell 2. The training phase is traditional, with orthogonal pilots reused in each cell. The data transmission phase is modified by the introduction of silences, referred to as blank subframes, where users within a same cell do not transmit. Blank subframes (with white background on figure) are pseudo-randomly and independently placed within each cell. As a consequence, it can occasionally occur that users of both cells remain silent during the same subframe.

where $\boldsymbol{C}_{\mathsf{y}|\mathsf{G}}$ is given in (17), and $\boldsymbol{C}_{\mathsf{y}'|\mathsf{G}'} := \mathbb{E}\{\, \mathbf{y}'\mathbf{y}'^\dagger | \mathsf{G}' \,\}$ is the covariance of the signal in (11), given by

$$\boldsymbol{C}_{\mathsf{y}'|\mathsf{G}'} = P\hat{\mathbf{G}}_1\hat{\mathbf{G}}_1^\dagger + P\tilde{\mathbf{G}}_1\tilde{\mathbf{G}}_1^\dagger + P\sum_{l>1}\mathbf{G}_l\mathbf{G}_l^\dagger + \boldsymbol{I}. \tag{26}$$

By combining (21), (23) and (25), we obtain the group-blind detector $\mathbf{w}_{1k}$, that is explicitly given by

$$\mathbf{w}_{1k} = \left\{\boldsymbol{I} - \breve{\mathbf{U}}_{\hat{\mathsf{G}}_1}\left(\breve{\mathbf{U}}_{\hat{\mathsf{G}}_1}^\dagger \boldsymbol{C}_{\mathsf{y}|\mathsf{G}}\breve{\mathbf{U}}_{\hat{\mathsf{G}}_1}\right)^{-1}\breve{\mathbf{U}}_{\hat{\mathsf{G}}_1}^\dagger \boldsymbol{C}_{\mathsf{y}'|\mathsf{G}'}\right\}\dot{\mathbf{w}}_{1k}. \tag{27}$$

Note that (27) can be applied to the case of cells with different number of users. Furthermore, it can be used in the presence of general estimation impairments as modeled by the error $\tilde{\mathbf{G}}_1$ and the imperfect estimate $\hat{\mathbf{G}}_1$.

The implementation of the detector in (27) requires the knowledge of $\boldsymbol{C}_{\mathsf{y}'|\mathsf{G}'}$, which is practically not available at the BS. While the analytical results in Section V assume the knowledge of $\boldsymbol{C}_{\mathsf{y}'|\mathsf{G}'}$, Section IV provides a method to obtain a practical approximation of $\boldsymbol{C}_{\mathsf{y}'|\mathsf{G}'}$, which is validated in Section VI.

IV. IMPLEMENTATION

The knowledge of $\boldsymbol{C}_{\mathsf{y}|\mathsf{G}}$ and $\boldsymbol{C}_{\mathsf{y}'|\mathsf{G}'}$ is needed to implement (25). In the below Section IV-A, we propose a method, which we refer to as *method of silences*, to obtain an approximation of $\boldsymbol{C}_{\mathsf{y}'|\mathsf{G}'}$ through the estimated aggregate out-of-cell channel covariance. With such estimation, a practical implementation is proposed in Section IV-B. The *method of silences* that we propose is practically implementable due to its resemblance to the Almost Blank Subframes technique in LTE [55], [61], [62]. This method is also capable of reaching a large fraction of the gain achievable with the ideal group-blind detector in several scenarios as shown in Section VI.

We note that the group-blind detector (27) can be applied to massive MIMO irrespective of the covariance estimation scheme, although any practical implementation, and so its performance, depends on the particular estimation chosen. A thorough analysis of general estimation methods is beyond the scope of this paper and is left as a future work.

A. Out-of-cell Channel Covariance Estimation

The method that follows, which we refer to as *method of silences*, is a data encoding that allows to derive an estimation of the aggregate out-of-cell channel covariance

$$\boldsymbol{\Sigma}_1 := \sum_{l>1}\mathbf{G}_l\mathbf{G}_l^\dagger. \tag{28}$$

During each coherence time of duration T, the frame of each user is partitioned into a training frame, of duration T_τ, and a data frame, of duration $T_{\mathsf{d}} = T - T_\tau$ (see Fig. 1). For clarity of exposition, let the data frame be divided into subframes (it will appear evident that this assumption is inessential). Each BS independently selects, uniformly at random, a subset of subframes during which users within its cell do not transmit.

Let α denote the fraction of blank subframes (silences). During a blank subframe, in-cell users are silent, and the signal received by the BS is the superposition of the signals transmitted by users in other cells. Users within each cell can be either silent (with probability α) or active (with probability $1-\alpha$). The received signal during blank subframes is

$$\mathbf{y}_* = \sum_{l>1}\mathsf{a}_l\mathbf{G}_l\mathbf{x}_l + \mathbf{n}, \tag{29}$$

where a_l models whether users in cell l are silent ($\mathsf{a}_l = 0$) or active ($\mathsf{a}_l = 1$). Since base stations do not cooperate, $\{\mathsf{a}_2, \ldots, \mathsf{a}_L\}$ are i.i.d. random variables; moreover, since cells choose the blank subframes uniformly at random, each variable a_l is Bernoulli distributed with probability of success $1-\alpha$. The covariance matrix $\boldsymbol{C}_{\mathsf{y}_*|\mathsf{G}} = \mathbb{E}\{\,\mathbf{y}_*\mathbf{y}_*^\dagger\,|\,\mathsf{G}\,\}$ of the received signal is

$$\begin{aligned}\boldsymbol{C}_{\mathsf{y}_*|\mathsf{G}} &= \sum_{l_1>1}\sum_{l_2>1}\mathbb{E}\{\,\mathsf{a}_{l_1}\mathsf{a}_{l_2}\,\}\,\mathbf{G}_{l_1}\mathbf{G}_{l_2}^\dagger P\delta_{l_1 l_2} + \boldsymbol{I}\\ &= (1-\alpha)P\sum_{l>1}\mathbf{G}_l\mathbf{G}_l^\dagger + \boldsymbol{I},\end{aligned} \tag{30}$$

hence, the aggregate out-of-cell channel covariance (28) can be retrieved as follows:

$$\boldsymbol{\Sigma}_1 = \frac{1}{(1-\alpha)P}(\boldsymbol{C}_{\mathsf{y}_*|\mathsf{G}} - \boldsymbol{I}). \tag{31}$$

Denote $\mathcal{T}_*$ the set of symbol periods during blank subframes. Replacing the covariance matrix $\boldsymbol{C}_{\mathsf{y}_*|\mathsf{G}}$ on the RHS of (31) with the sample-covariance

$$\hat{\boldsymbol{C}}_{\mathsf{y}_*|\mathsf{G}} = \frac{1}{\alpha T_{\mathsf{d}}}\sum_{m\in\mathcal{T}_*}\mathbf{y}_*(m)\mathbf{y}_*(m)^\dagger \tag{32}$$

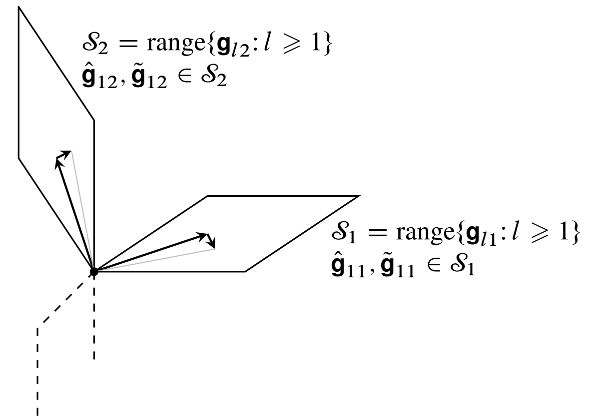

FIG. 2: Conceptual representation of the signal space in the massive regime with negligible effect of noise during training ($\epsilon = 0$). Channels are asymptotically orthogonal in the a.s. sense; however, for fixed in-cell user j, both estimated and error vectors lie in $\mathcal{S}_j = \text{range}\{\mathbf{g}_{lj}: l \geqslant 1\}$. Although their projections onto vectors in $\mathcal{S}_j$ do not vanish in general, projections onto vectors in $\mathcal{S}_k$, $k \neq j$, do vanish.

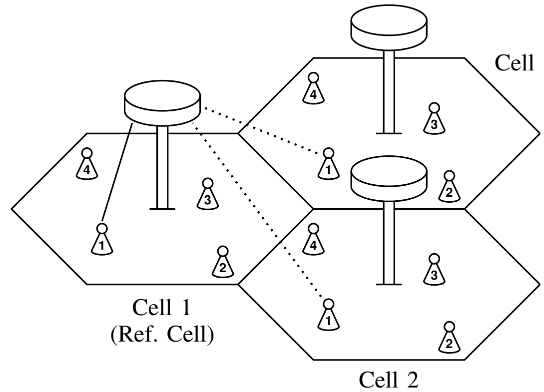

FIG. 3: Interference in the massive regime. During the training phase, the signal received from each in-cell user is corrupted by the interference of one user only per interfering cell (users with label 1), which causes pilot contamination. Remaining users (labels different from 1) are nulled since pilots are orthogonal. During the data transmission phase, the same subset of out-of-cell users that caused pilot contamination interferes, while interference from other users asymptotically vanishes.

results in the following estimation of $\mathbf{\Sigma}_1$:

$$\hat{\mathbf{\Sigma}}_1 = \frac{1}{(1-\alpha)P}(\hat{\boldsymbol{C}}_{\mathsf{y}_*|\mathsf{G}} - \boldsymbol{I}). \tag{33}$$

B. Detector Implementation

In order to implement $\mathbf{w}_{1k}$ in (27), the BS requires the knowledge of $\boldsymbol{C}_{\mathsf{y}'|\mathsf{G}'}$ and $\boldsymbol{C}_{\mathsf{y}|\mathsf{G}}$. We below discuss approximations of $\boldsymbol{C}_{\mathsf{y}'|\mathsf{G}'}$ and $\boldsymbol{C}_{\mathsf{y}|\mathsf{G}}$ that can be practically obtained.

Approximation 1. The covariance matrix $\boldsymbol{C}_{\mathsf{y}'|\mathsf{G}'}$ can be approximated as follows:

$$\boldsymbol{C}_{\mathsf{y}'|\mathsf{G}'} \approx \boldsymbol{C}^{\circ}_{\mathsf{y}'|\mathsf{G}'} = P\hat{\mathbf{G}}_1\hat{\mathbf{G}}_1^{\dagger} + P\hat{\mathbf{\Sigma}}_1 + \boldsymbol{I}, \tag{34}$$

where $\hat{\mathbf{\Sigma}}_1$ is obtained in (33) via the *method of silences*, and $\hat{\mathbf{G}}_1$ is obtained via the training phase.

The above approximation follows from the fact that $\boldsymbol{C}_{\mathsf{y}'|\mathsf{G}'}$ is postmultiplied by $\dot{\mathbf{w}}_{1k} \in \text{range}\{\hat{\mathbf{G}}_1\}$, and $n^{-1}\tilde{\mathbf{G}}_1^{\dagger}\dot{\mathbf{w}}_{1k} \xrightarrow{\text{a.s.}} \mathbf{0}$ (cf. (27)).

Approximation 2. The covariance matrix $\boldsymbol{C}_{\mathsf{y}|\mathsf{G}}$ can be approximated as follows:

$$\boldsymbol{C}_{\mathsf{y}|\mathsf{G}} \approx \boldsymbol{C}^{\circ}_{\mathsf{y}|\mathsf{G}} = \frac{1}{1-\alpha}[\hat{\boldsymbol{C}}^{\text{ABS}}_{\mathsf{y}} - \alpha \boldsymbol{I}] \tag{35}$$

where $\hat{\boldsymbol{C}}^{\text{ABS}}_{\mathsf{y}}$ is the covariance

$$\hat{\boldsymbol{C}}^{\text{ABS}}_{\mathsf{y}} = \frac{1}{T_{\mathsf{d}}}\sum_{m=1}^{T_{\mathsf{d}}} \mathbf{y}(m)\mathbf{y}(m)^{\dagger}, \tag{36}$$

and both (35) and (36) take into account the presence of silences during the data transmission phase. The derivation of (35) follows an approach similar to (30).

Using Approximations 1 and 2 in (27) yields the following implementation form of the group-blind detector:

$$\mathbf{w}^{\circ}_{1k} = \left\{\boldsymbol{I} - \breve{\mathbf{U}}_{\hat{\mathbf{G}}_1}\left(\breve{\mathbf{U}}^{\dagger}_{\hat{\mathbf{G}}_1}\boldsymbol{C}^{\circ}_{\mathsf{y}|\mathsf{G}}\breve{\mathbf{U}}_{\hat{\mathbf{G}}_1}\right)^{-1}\breve{\mathbf{U}}^{\dagger}_{\hat{\mathbf{G}}_1}\boldsymbol{C}^{\circ}_{\mathsf{y}'|\mathsf{G}'}\right\}\dot{\mathbf{w}}_{1k}. \tag{37}$$

Denote γ°_{1k} the SINR achieved with $\mathbf{w}^{\circ}_{1k}$. The performance of $\mathbf{w}^{\circ}_{1k}$ depends on the accuracy of the estimation $\hat{\mathbf{\Sigma}}_1$, which in turn depends on α for fixed T_{d}, i.e., $\gamma^{\circ}_{1k} = \gamma^{\circ}_{1k}(\alpha)$. In terms of achievable rate, the optimum α is the one that maximizes the *net achievable rate* $(1-\alpha)R_{1k}(\alpha)$, where $R_{1k}(\alpha) = \mathbb{E}\{\log(1+\gamma^{\circ}_{1k})\}$.

V. Asymptotic Analysis

In this section we derive analytical results for the asymptotic SINR gain achieved by the proposed group-blind detector in the massive regime, i.e., for $n \to \infty$ while keeping K and L finite. We give preliminary properties in Section V-A. Then in Section V-B we study in detail a scenario with one dominant interfering cell that takes into account the effect of noise during training. Finally, in Section V-C we consider the general multicell scenario in the high-SNR regime.

A. Preliminaries

A first important observation in the analysis of the massive regime is that the effect of any uncorrelated noise vanishes in the limit of an infinite number of antennas [11]. Therefore, only non-vanishing interfering terms after detection can bound the SINR, and it is natural to consider the network as interference-limited. The following two properties of channels are at the basis of our asymptotic results:

i) As $n \to \infty$ with K and L finite, channels become asymptotically orthogonal in the a.s. sense, i.e., $n^{-1}\mathbf{g}^{\dagger}_{kl}\mathbf{g}_{k'l'} \xrightarrow{\text{a.s.}} \beta_{kl}\delta_{kk'}\delta_{ll'}$;
ii) In the limit of infinite effective-training SNR, i.e., $\epsilon = 0$, it results $\hat{\mathbf{g}}_{1k} \in \mathcal{S}_k := \text{range}\{\mathbf{g}_{lk}: l \geqslant 1\}$ (cf. (6)).

Due to i), the following limit holds:

$$\frac{1}{n}\hat{\mathbf{g}}^{\dagger}_{1k}\mathbf{g}_{lj} = \frac{1}{n}\varphi_{1k}\beta^{-1}_{1k}\left(\sum_{m\geqslant 1}\mathbf{g}^{\dagger}_{mk} + \sqrt{\epsilon}\mathbf{v}^{\dagger}_{1k}\right)\mathbf{g}_{lj}$$

$$\xrightarrow{\text{a.s.}} \varphi_{1k}\beta_{1k}^{-1}\beta_{lj}\delta_{kj}. \tag{38}$$

A conceptual representation for the structure of the signal space in the massive regime when $\epsilon = 0$ is shown in Fig. 2. Asymptotically, the signal space $\mathcal{S} = \text{range}\{\mathbf{G}_1, \mathbf{G}_2, \dots, \mathbf{G}_L\}$ is the direct sum of the K subspaces $\{\mathcal{S}_k\}_{k=1}^K$, $\mathcal{S} = \mathcal{S}_1 \oplus \mathcal{S}_2 \oplus \dots \oplus \mathcal{S}_K$, each of which is spanned by $\{\mathbf{g}_{1k}, \mathbf{g}_{2k}, \dots, \mathbf{g}_{Lk}\}$. As a consequence, in-cell user k is asymptotically interfered by out-of-cell users who used the same training sequence only (see Fig. 3). A similar conclusion, namely that in-cell user k is not affected by user $j \neq k$ in other cells, remains true with the proposed detector (cf. (27)), as proven in the below lemma.

Lemma 1. Denote $z_{1k} = n^{-1}\mathbf{w}_{1k}^\dagger \mathbf{y}'$ the variable after detection normalized to the number of antennas. The following asymptotic relation holds:

$$z_{1k} \asymp \frac{1}{n}\mathbf{w}_{1k}^\dagger \hat{\mathbf{g}}_{1k} \mathsf{x}_{1k} + \frac{1}{n}\mathbf{w}_{1k}^\dagger \tilde{\mathbf{g}}_{1k} \tilde{\mathsf{x}}_{1k} + \sum_{l>1} \frac{1}{n}\mathbf{w}_{1k}^\dagger \mathbf{g}_{lk} \mathsf{x}_{lk} + \frac{1}{n}\mathbf{w}_{1k}^\dagger \mathbf{n}. \tag{39}$$

Proof: See Appendix A. □

We refer to the case where $\breve{\mathbf{w}}_{1k} = \mathbf{0}$ and $\dot{\mathbf{w}}_{1k}$ is a linear detector (MF, MMSE, or RZF) as non-group-blind detection. In order to compare group-blind (GB) vs. non-group-blind (NGB) detection, we will investigate the following metric of interest.

Definition 1. The *asymptotic SINR gain* provided by group-blind detection is

$$\bar{\eta}_{1k} = \frac{\bar{\gamma}_{1k}}{\bar{\gamma}_{1k}^{\mathsf{NGB}}}, \tag{40}$$

where $\bar{\gamma}_{1k}$ and $\bar{\gamma}_{1k}^{\mathsf{NGB}}$ are the asymptotic SINRs achieved by the proposed group-blind detector and by non-group-blind detectors, respectively.

The asymptotic SINR achieved with non-group-blind detectors is [11], [25]:

$$\bar{\gamma}_{1k}^{\mathsf{NGB}} := \frac{\beta_{1k}^2}{\sum_{l>1}\beta_{lk}^2}. \tag{41}$$

B. Performance with One Dominant Interfering Cell

We now consider the case $L = 2$ to model a scenario with one dominant interfering cell. In this case, the variable after detection is (cf. (39)):

$$z_{1k} \asymp \frac{1}{n}\mathbf{w}_{1k}^\dagger \hat{\mathbf{g}}_{1k} \mathsf{x}_{1k} + \frac{1}{n}\mathbf{w}_{1k}^\dagger \tilde{\mathbf{g}}_{1k} \tilde{\mathsf{x}}_{1k} + \frac{1}{n}\mathbf{w}_{1k}^\dagger \mathbf{g}_{2k} \mathsf{x}_{2k} + \frac{1}{n}\mathbf{w}_{1k}^\dagger \mathbf{n}. \tag{42}$$

The SINR corresponding to the variable z_{1k} is provided by the following theorem.

Theorem 1. Let $L = 2$. The following asymptotic SINR $\bar{\gamma}_{1k}$ for user k is achievable with group-blind detection:

$$\bar{\gamma}_{1k} = \left[1 + \frac{1}{(1+\epsilon/\beta_{2k})^2}\right]\frac{\beta_{1k}^2}{\beta_{2k}^2}. \tag{43}$$

Proof: See Appendix B. □

The following corollary results from Theorem 1.

Corollary 1. Let $L = 2$. The following asymptotic SINR gain for user k is achievable by group-blind detection:

$$\bar{\eta}_{1k} = 1 + \frac{1}{(1+\epsilon/\beta_{2k})^2}. \tag{44}$$

Proof: The result follows from (43) and by noticing that $\bar{\gamma}_{1k}^{\mathsf{NGB}} = \beta_{1k}^2/\beta_{2k}^2$ from (41). □

Both the asymptotic SINR $\bar{\gamma}_{1k}$ and the gain $\bar{\eta}_{1k}$ simplify in the limit $\epsilon \to 0$, as specified in the corollary that follows.

Corollary 2. Let $L = 2$ and $\epsilon \to 0$. The following asymptotic SINR $\bar{\gamma}_{1k}$ for user k is achievable by group-blind detection:

$$\bar{\gamma}_{1k} \to 2\bar{\gamma}_{1k}^{\mathsf{NGB}}, \tag{45}$$

and the following limit holds for the asymptotic SINR gain:

$$\bar{\eta}_{1k} \to 2. \tag{46}$$

Proof: By assuming $\epsilon \ll \beta_{2k}$, $\bar{\eta}_{1k}$ can be expanded as $\bar{\eta}_{1k} = 2 - 2\epsilon/\beta_{2k} + O(\epsilon^2)$, whence the result. □

The above corollary shows that, in the high-SNR regime, the asymptotic SINR achieved with group-blind detection is doubled compared to traditional detection.

Let $\Delta\bar{R}_{1k}$ be the *rate gap* defined as the difference between the asymptotic rates achieved by user k with and without group-blind detection:

$$\Delta\bar{R}_{1k} = \log(1+\bar{\gamma}_{1k}) - \log(1+\bar{\gamma}_{1k}^{\mathsf{NGB}}). \tag{47}$$

In the high-SNR regime, the value of $\Delta\bar{R}_{1k}$ can be approximated as specified in the following remark.

Remark 2. We substitute (41) and (43) in (47), and consider the two extreme cases of weak and strong out-of-cell interference, given by $\beta_{2k} \ll \beta_{1k}$ and $\beta_{2k} \gg \beta_{1k}$, respectively. In the presence of weak out-of-cell interference, the rate gap is given by $\Delta\bar{R}_{1k} \approx 1$ bits/s/Hz. In the presence of strong out-of-cell interference, the rate gap is $\Delta\bar{R}_{1k} \approx \bar{\gamma}_{1k}^{\mathsf{NGB}}\log_2 e$ bits/s/Hz. Note that the case $\beta_{2k} \gg \beta_{1k}$ can occur when BSs are irregularly deployed.

C. High-SNR Performance with Multiple Interfering Cells

In this subsection, we consider the general case of multiple interfering cells, i.e., $L \geqslant 2$. We assume sufficiently large SNR during the training phase, which requires $\epsilon \ll \sum_{l\geqslant 1}\beta_{lk}$ (cf. (7)). Similarly, for a sufficiently large number of antennas the data transmission phase falls in the high-SNR regime [11]. Therefore, we consider the scenario with multiple interfering cells as interference limited, and we neglect ϵ in the remainder of the subsection.

Theorem 2. Let $L \geqslant 2$ and $\epsilon = 0$. The following asymptotic SINR $\bar{\gamma}_{1k}$ for user k is achievable with group-blind detection:

$$\bar{\gamma}_{1k} = L\beta_{1k}^2 \Bigg/ \left\{\sum_{l=2}^{L}\beta_{lk}\right\}^2. \tag{48}$$

Proof: See Appendix C. □

The proof unveils the effect of group-blind detection: while a non-group-blind detector simply removes the self-interference term originated from $\tilde{\mathbf{G}}_1$, the group-blind detector (cf. (27)) allows to partially introduce self-interference in the decoder in exchange for reducing out-of-cell interference (cf. (77)). The latter achieves the optimum trade-off by minimizing the MSE in (16), as verified in Appendix D.

Remark 3. Theorem 2 holds in the massive regime, i.e., as $n \to \infty$ while keeping K and L finite. From property i) in Section V-A, this holds in practice when $n \gg LK$, and thus when the number of interfering cells satisfies $L \ll n/K$. We note that this would be the case in massive MIMO systems since the number of significant interfering cells L is bounded in practice from physical considerations while n is sufficiently large.

Remark 4. There exist sequences $(\beta_{lk})_{l\geqslant 1}$ such that the asymptotic SINR $\bar{\gamma}_{1k}$ is a non-monotonic function of L. This does not imply that *capacity* is non-monotonic as well. In fact, for any user k, we consider, in line with the literature (e.g. [11], [25], [56]), an *achievable rate* that lower bounds and should not be regarded as an approximation of capacity. The reader is referred to [63] for results on capacity of MIMO systems in Rayleigh fading. Capacity of spatially and doubly correlated MIMO channels can be found in [64] and [65], respectively. A specific investigation of capacity in mobile communications can be found in [66]. Outage capacity is studied in [67]. An investigation on the reliability-rate tradeoff is reported in [68].

The following corollary follows from Theorem 2 by using (48) and (41) in (40).

Corollary 3. Let $L \geqslant 2$ and $\epsilon = 0$. The following asymptotic SINR gain for user k is achievable by group-blind detection:

$$\bar{\eta}_{1k} = L \sum_{l>1} \beta_{lk}^2 \bigg/ \left\{ \sum_{l>1} \beta_{lk} \right\}^2. \tag{49}$$

Note that $\bar{\eta}_{1k}$ does not depend on β_{1k}. The extrema of $\bar{\eta}_{1k}$ as a function of $\{\beta_{lk}\}_{l\geqslant 1}$ are as follows:

$$\frac{L}{L-1} = \bar{\eta}_{\mathsf{min}} \leqslant \bar{\eta}_{1k} \leqslant \bar{\eta}_{\mathsf{max}} = L, \tag{50}$$

where the minimum is achieved when $\beta_{2k} = \cdots = \beta_{Lk}$ and the maximum is achieved when only one element in $\{\beta_{2k}, \ldots, \beta_{Lk}\}$ is nonzero. It should be noted that the latter is achievable in a limit sense, as $\{\beta_{lk}\}$ are assumed strictly positive. Following the argument in Remark 3, L is in practice finite. Therefore, $\bar{\eta}_{\mathsf{max}}$ is bounded as well, and $\bar{\eta}_{\mathsf{min}}$ is bounded away from unity.

VI. Numerical Results

We provide in the below Section VI-A numerical results to validate our analytical results and confirm the performance gain provided by the proposed group-blind detector with respect to non-group-blind detectors in realistic scenarios. Moreover, in Section VI-B we evaluate the performance of the group-blind detector when it is implemented jointly with the *method of silences*, showing that a large fraction of the promised gain can be achieved.

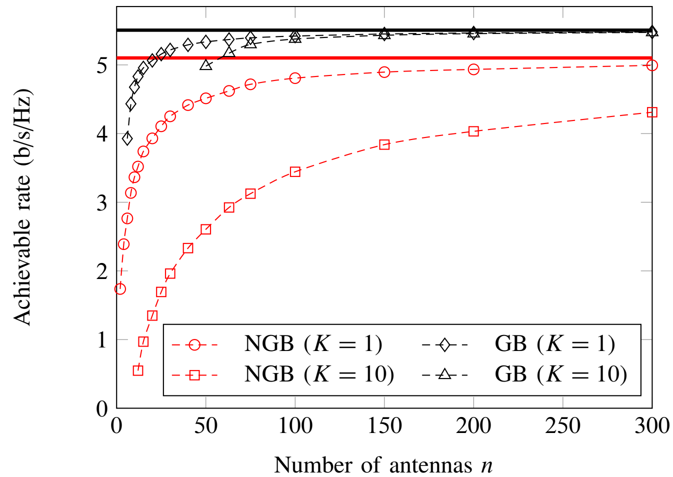

FIG. 4: Achievable rate (b/s/Hz) with group-blind (GB) and non-group-blind (NGB) detection with $L = 4$ cells, and either $K = 1$ or $K = 10$ users per cell. Users within the reference cell are received with $\mathrm{SNR} = 10$ dB. Users in adjacent cells are attenuated by 10 dB.

Hereinafter in this section, we consider β_{lj} constant with respect to j, that is, users within a given cell are received with same average power, which depends on the cell only. Within the reference cell, we set $\beta_{1k} = 1$, hence $\mathrm{SNR} = P$, irrespective of the particular user considered. Unless otherwise stated, we set $\epsilon = 0$ and consider MMSE detectors when plotting curves for traditional (i.e., non-group-blind) detection. On all figures, dashed lines connect points obtained via numerical simulations, while solid lines are obtained from closed form expressions. Asymptotic achievable rates are shown with horizontal solid lines.

A. Analysis Validation and Performance Gain

We start by comparing the rate achievable with and without group-blind detection in Fig. 4. We consider a scenario with $L = 4$ cells, $\mathrm{SNR} = 10$ dB, and a number of users per cell equal to either $K = 1$ or $K = 10$. Fig. 4 shows the achievable rate R_{1k} (cf. (9)) as a function of the number of antennas n. GB detection is showed for $n \geqslant KL$, which is the required minimum number of antennas to properly implement the detector. Figure 4 confirms the accuracy of the asymptotic results given in Section V. Moreover, the figure shows that GB detection outperforms NGB detection, and is more robust to variations of the network load, i.e., the number of users per BS antenna.

In Fig. 5, we consider a more involved scenario with a section of a hexagonal lattice with several concentric rings of cells arranged around the reference cell. Ring r contains $6r$ cells, and cells are labeled from inner to outer rings. Cells with labels $2 + 3(r-1)r \leqslant l \leqslant 1 + 3r(r+1)$ lie in ring r. Cell organization and labeling is shown in Fig. 6. Users are attenuated according to a pathloss model with pathloss exponent equal to $\alpha_{\mathrm{pl}} = 3.7$. Distance between cell centers is normalized to one: out-of-cell users are placed at the cell center, while in-cell users are placed on a circle with radius d_{in}. Therefore, for $l \in [2 + 3(r-1)r, 1 + 3r(r+1)]$ with $r \geqslant 1$, it results $\beta_{lk} = r^{-\alpha_{\mathrm{pl}}/2}/d_{\mathrm{in}}^{-\alpha_{\mathrm{pl}}/2}$, while $\beta_{1k} = 1$. We

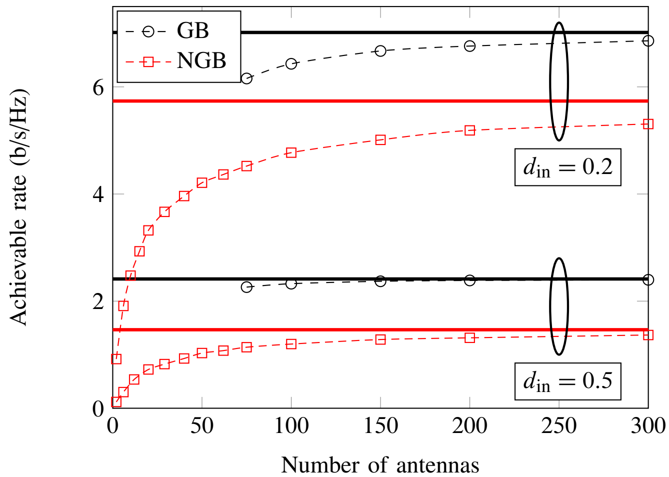

FIG. 5: Achievable rate (b/s/Hz) as a function of the number of antennas n with $r = 4$ rings of hexagonal cells centered around the reference cell, $K = 1$, SNR $= 10$ dB, and two different positions of the in-cell user, that is placed either near the cell center ($d_{\text{in}} = 0.2$) or the cell edge ($d_{\text{in}} = 0.5$). The two positions correspond to weak and strong interference scenarios, respectively.

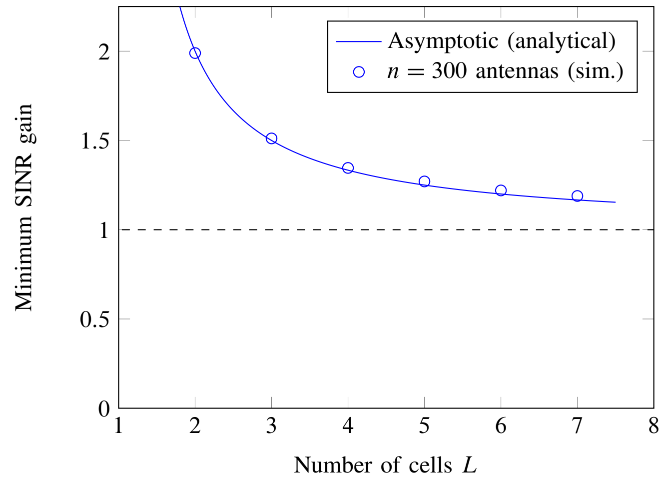

FIG. 7: Minimum SINR gain η_{min} as a function of the number of cells L. Theoretical asymptotic gain (solid line) and numerical simulations (points) with $n = 300$ are compared.

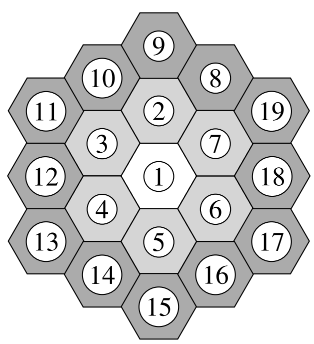

FIG. 6: Hexagonal cell section and labeling. The reference cell is labeled 1. Two rings of concentric cells are shown with different gray levels. Labels referring to cells in the inner and outer rings belong to $[2 : 7]$ and $[8 : 19]$, respectively.

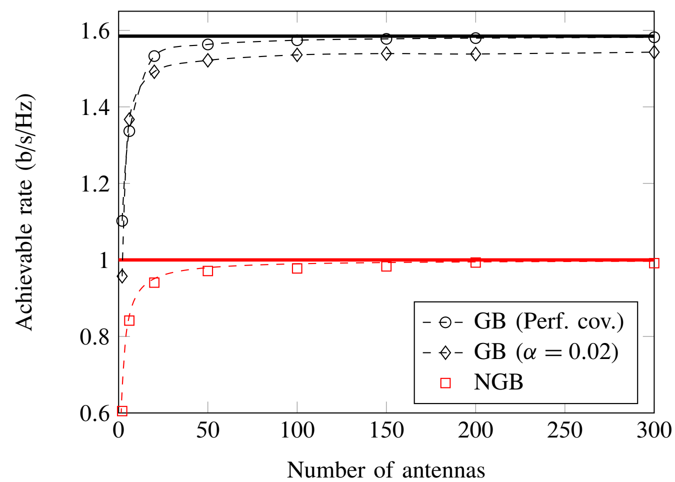

FIG. 8: Achievable rate (b/s/Hz) as a function of the number of antennas n with $L = 2$, $K = 1$, SNR $= 20$ dB, and $\beta_{11}/\beta_{21} = 0$ dB (strong interference).

set $P = 10$, hence the received SNR is fixed to 10 dB, but the interference power depends on the distance d_{in} of the in-cell user from the BS. Fig. 5 shows the achievable rate as a function of the number of antennas with NGB and GB receivers, for two scenarios corresponding to in-cell user near either the cell center ($d_{\text{in}} = 0.2$) or the cell edge ($d_{\text{in}} = 0.5$). In both cases, we find a significant rate gain and a fast convergence towards the asymptotic rate as the number of antennas grows.

Figure 7 shows the SINR gain η_{1k} as a function of the number of cells L obtained by the GB detector with respect to traditional NGB detectors in a scenario with $\beta_{2k} = \beta_{3k} = \cdots = \beta_{Lk}$. The considered scenario yields the minimum asymptotic SINR obtainable by the GB detector (cf. (50)). The asymptotic minimum SINR gain (solid line) is compared to numerical simulations (points) with $n = 300$ antennas at the BS. Even in the worst case scenario, GB detection outperforms NGB detection, and the analytical lower bound in (50) tightly approximates simulations.

B. *Performance with the Method of Silences*

We consider in Fig. 8 a scenario with $L = 2$, $K = 1$, SNR $= 20$ dB, and $\beta_{11}/\beta_{21} = 0$ dB (strong interference). We compare the achievable rate with traditional detection (MF) and GB detection, with both perfect $\mathbf{\Sigma}_1$ and estimated $\hat{\mathbf{\Sigma}}_1$ with $\alpha = 0.02$. In accordance with eqs. (41), (45), and (47), GB detection outperforms NGB detection by $\Delta\bar{R}_{1k} = \log_2(1+2\cdot 1) - \log_2(1+1) \approx 0.585$ b/s/Hz. It is also shown that the loss incurred by using the *method of silences* is small compared to the rate gap between GB and NGB detection.

Dependence of the net achievable rate on the blocklength is depicted in Fig. 9, where the net achievable rate is shown as a function of the silence fraction α, for the two blocklengths $T_{\text{d}} = 500$ and $T_{\text{d}} = 1000$ symbols. We interpret $T_{\text{d}} = 500$ symbols as a realistic blocklength (e.g. blocklength equal to 550 symbols for users moving at 250 km/h is derived in [69, Section IV-B]) and $T_{\text{d}} = 1000$ symbols as corresponding to a more optimistic scenario. Other parameters are the same as in Fig. 8. It is shown that there exists an optimum silence

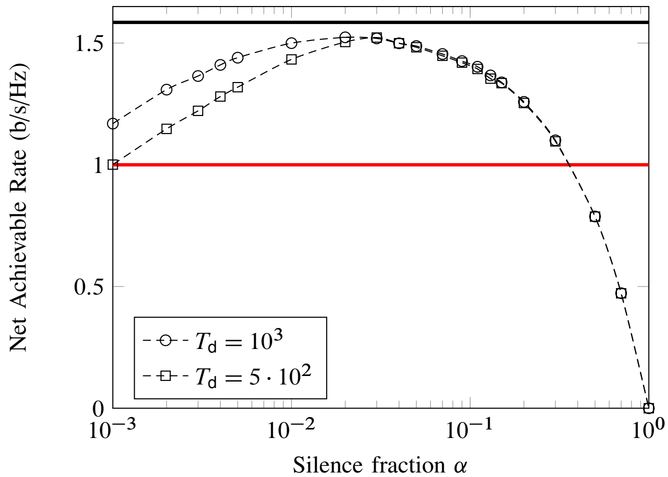

FIG. 9: Net achievable rate (b/s/Hz) as a function of the fraction of silence α, for two values of the blocklength T_d. Scenario parameters: $L = 2$, $K = 1$, SNR $= 20$ dB, and $\beta_{11}/\beta_{21} = 0$ dB (strong interference).

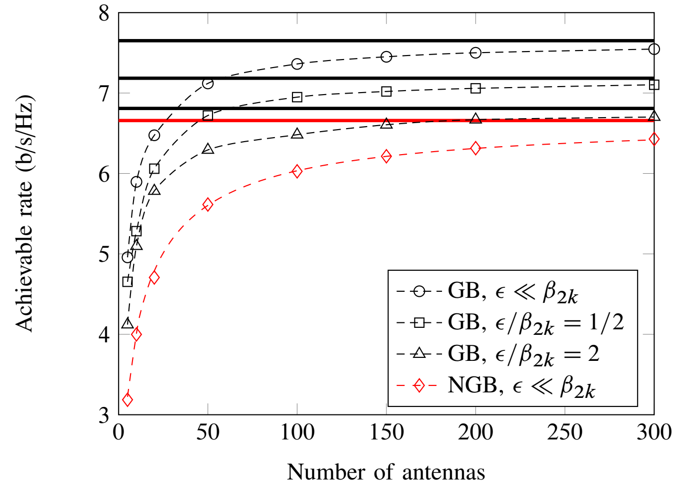

FIG. 10: Achievable rate (b/s/Hz) as a function of the number of antennas, in presence of non-neglibile noise effects during the training phase. Scenario parameters: $L = 2$, $K = 1$, SNR $= 10$ dB, and $\beta_{11}/\beta_{21} = 10$ dB.

fraction α (cf. Section IV-B), and that the *method of silences* is good enough to ensure a positive rate gap with respect to NGB detection for practical blocklengths corresponding to coherence times in the order of the milliseconds. We also note that the net rate does not appear to be very sensitive to the blocklength and thus to the coherence time, as long as a suitable value for α is chosen.

Figure 10 shows the achievable rate R_{1k} vs. the number of antennas n for GB detection. We consider several values of ϵ/β_{2k}, that model whether the estimation error is dominated by pilot contamination ($\epsilon < \beta_{2k}$) or by thermal noise ($\epsilon > \beta_{2k}$). Scenario parameters are as follows: $L = 2$, $K = 1$, SNR $= 10$ dB, and fixed β_{21} with $\beta_{11}/\beta_{21} = 10$ dB (weak interference). The rate achieved by the NGB detector in the presence of negligible noise during the training phase is plotted for comparison. The rate achieved with GB detectors decreases as ϵ grows, consistently with (43). However, even when the training phase is severely affected by noise, GB detection still outperforms NGB detection with noise-free training phase. Finally, consistently with Remark 2 for the case of weak out-of-cell interference, Fig. 10 shows a rate gap $\Delta\bar{R}_{1k} \approx 1$ b/s/Hz between GB and NGB with negligible noise, i.e., $\epsilon \ll \beta_{2k}$.

VII. Conclusion

We proposed a group-blind detector for the uplink of massive MIMO that takes into account the presence of pilot contamination and achieves higher rates than those attained with traditional detectors. We derived analytical results for asymptotic SINR and achievable rate with unlimited number of antennas and verified our findings through simulations. We showed, in particular, that group-blind detection outperforms traditional detection and is more robust to variations of the network load. Numerical results suggested that the gap between asymptotic and non-asymptotic rates depends on both SNR and number of antennas, and can be negligible in practical scenarios.

The major novel component of the proposed group blind detector is a correction filter which exploits the excess degrees of freedom provided by the large number of antennas per BS in order to reduce interference. The implementation of the group-blind detector necessitates the knowledge of the aggregate instantaneous out-of-cell channel covariance. We proposed a method, which we referred to as *method of silences*, to address this implementation issue. The method of silences introduces blank subframes within the data transmission phase, and allows each BS to estimate the required second-order statistics during such subframes. We showed via simulations that this method achieves a large fraction of the promised SINR gain in scenarios of interest.

There are several possible extensions of this work. From a channel model perspective, it is desirable to account for the effect of antenna correlation and finite number of degrees of freedom. In fact, massive MIMO may suffer from an inherent problem of spatial correlation among BS antennas due to lack of sufficient spacing among them. From an information-theoretic standpoint, it is useful to understand the fundamental limits of detection in the massive regime. Since our detector was derived by maximizing a traditional lower bound on capacity, rates higher than those presented could be achievable. From a system implementation perspective, an analytical study of the gap between ideal and implemented detectors is of interest. More generally, practical solutions other than the *method of silences* as well as different training phase designs with non-orthogonal pilots are possible, and their investigation can be regarded as a future research direction.

Appendix A
Proof of Lemma 1

Proof: We prove that $n^{-1}\mathbf{w}_{1k}^{\dagger}\mathbf{g}_{lj} \xrightarrow{\text{a.s.}} 0$ for $j \neq k$ by using expanding $\mathbf{w}_{1k}$ in terms of $\dot{\mathbf{w}}_{1k}$ and $\breve{\mathbf{w}}_{1k}$ (cf. (21)) and showing that $n^{-1}\dot{\mathbf{w}}_{1k}^{\dagger}\mathbf{g}_{lj}$ and $n^{-1}\breve{\mathbf{w}}_{1k}^{\dagger}\mathbf{g}_{lj}$ converge a.s. to zero for $j \neq k$. First note that (23) implies

$$\frac{1}{n}\dot{\mathbf{w}}_{1k}^{\dagger}\mathbf{g}_{lj} \xrightarrow{\text{a.s.}} 0,\ \ j \neq k. \tag{51}$$

In order to show that

$$\frac{1}{n}\breve{\mathbf{w}}_{1k}^{\dagger}\mathbf{g}_{lj} \xrightarrow{\text{a.s.}} 0,\ \ j \neq k, \tag{52}$$

we decompose, without loss of generality, $\breve{\mathbf{w}}_{1k}$ as $\breve{\mathbf{w}}_{1k} = \breve{\mathbf{w}}_{1k}^{\parallel}+\breve{\mathbf{w}}_{1k}^{\perp}$, where $\breve{\mathbf{w}}_{1k}^{\parallel}$ is inside $\mathcal{S}_k$, i.e., $\breve{\mathbf{w}}_{1k}^{\parallel} \in \mathrm{range}\{\hat{\mathbf{g}}_{1k}\}^{\perp}\cap \mathcal{S}_k$, and $\breve{\mathbf{w}}_{1k}^{\perp}$ is orthogonal to $\mathcal{S}_k$, i.e., $\breve{\mathbf{w}}_{1k}^{\perp} \in \mathrm{range}\{\hat{\mathbf{g}}_{1k}\}^{\perp} \cap (\mathcal{S}_1 \oplus \cdots \oplus \mathcal{S}_{k-1} \oplus \mathcal{S}_{k+1} \oplus \cdots \oplus \mathcal{S}_K)$. We have that $n^{-1}\breve{\mathbf{w}}_{1k}^{\parallel\dagger}\mathbf{g}_{lj} \xrightarrow{\text{a.s.}} 0$ and $n^{-1}\breve{\mathbf{w}}_{1k}^{\perp\dagger}\mathbf{g}_{lj} \xrightarrow{\text{a.s.}} 0$ from the orthogonality of $\mathcal{S}_k$ and $\mathcal{S}_j$ when $j \neq k$, and from the MMSE-based design of the detector, respectively. The above implies (52). The lemma then follows from (51), (52), (21) and the definition of z_{1k} in the statement. □

Appendix B
Proof of Theorem 1

Proof: In the case $L = 2$, the matrix $\breve{\mathbf{U}}_{\hat{\mathbf{G}}_1}$ reduces to a unit-norm vector that is orthogonal to $\hat{\mathbf{g}}_{1k}$. Since $\tilde{\mathbf{g}}_{1k}$ is also asymptotically orthogonal to $\hat{\mathbf{g}}_{1k}$ by virtue of the orthogonality principle, we replace $\breve{\mathbf{U}}_{\hat{\mathbf{G}}_1}$ with $\hat{\mathbf{g}}_{1k}$. Hence, (25) becomes

$$\breve{\mathbf{w}}_{1k} \asymp -\frac{\tilde{\mathbf{g}}_{1k}\tilde{\mathbf{g}}_{1k}^{\dagger}}{\tilde{\mathbf{g}}_{1k}^{\dagger}\boldsymbol{C}_{\mathsf{y}'|\mathsf{G}'}\tilde{\mathbf{g}}_{1k}}\boldsymbol{C}_{\mathsf{y}'|\mathsf{G}'}\dot{\mathbf{w}}_{1k}. \tag{53}$$

The following limit holds for the denominator of (53):

$$\begin{aligned}\frac{1}{n^2}\tilde{\mathbf{g}}_{1k}^{\dagger}\boldsymbol{C}_{\mathsf{y}'|\mathsf{G}'}\tilde{\mathbf{g}}_{1k} &\asymp \frac{1}{n^2}\tilde{\mathbf{g}}_{1k}^{\dagger}(P\tilde{\mathbf{g}}_{1k}\tilde{\mathbf{g}}_{1k}^{\dagger} + P\mathbf{g}_{2k}\mathbf{g}_{2k})\tilde{\mathbf{g}}_{1k}\\ &\xrightarrow{\text{a.s.}} P(\beta_{1k}-\varphi_{1k})^2 + P(\varphi_{1k}\beta_{1k}^{-1}\beta_{2k})^2 =: \lambda P,\end{aligned} \tag{54}$$

with $\lambda = (\beta_{1k} - \varphi_{1k})^2 + (\varphi_{1k}\beta_{1k}^{-1}\beta_{2k})^2$. Since $\dot{\mathbf{w}}_{1k}$ is asymptotically proportional to $\hat{\mathbf{g}}_{1k}$ and the proportionality constant is inessential, we set $\dot{\mathbf{w}}_{1k} = \hat{\mathbf{g}}_{1k}$; (53) results in

$$\breve{\mathbf{w}}_{1k} \asymp -\frac{1}{n^2}\cdot\frac{1}{\lambda P}\tilde{\mathbf{g}}_{1k}\tilde{\mathbf{g}}_{1k}^{\dagger}\boldsymbol{C}_{\mathsf{y}'|\mathsf{G}'}\hat{\mathbf{g}}_{1k}. \tag{55}$$

Expanding $\mathbf{w}_{1k} = \dot{\mathbf{w}}_{1k} + \breve{\mathbf{w}}_{1k}$ in (42) and discarding terms that vanish due to asymptotic orthogonality yields:

$$\begin{aligned}z_{1k} \asymp &\frac{1}{n}\hat{\mathbf{g}}_{1k}^{\dagger}\hat{\mathbf{g}}_{1k}\mathsf{x}_{1k} + \frac{1}{n}\hat{\mathbf{g}}_{1k}^{\dagger}\mathbf{g}_{2k}\mathsf{x}_{2k}\\ &+\frac{1}{n}\breve{\mathbf{w}}_{1k}^{\dagger}\tilde{\mathbf{g}}_{1k}\tilde{\mathsf{x}}_{1k} + \frac{1}{n}\breve{\mathbf{w}}_{1k}^{\dagger}\mathbf{g}_{2k}\mathsf{x}_{2k}.\end{aligned} \tag{56}$$

Terms in (56) satisfy:

$$\frac{1}{n}\hat{\mathbf{g}}_{1k}^{\dagger}\hat{\mathbf{g}}_{1k} \xrightarrow{\text{a.s.}} \varphi_{1k}, \tag{57}$$

$$\frac{1}{n}\hat{\mathbf{g}}_{1k}^{\dagger}\mathbf{g}_{2k} \xrightarrow{\text{a.s.}} \varphi_{1k}\beta_{1k}^{-1}\beta_{2k}, \tag{58}$$

$$\frac{1}{n}\breve{\mathbf{w}}_{1k}^{\dagger}\tilde{\mathbf{g}}_{1k} \xrightarrow{\text{a.s.}} \lambda^{-1}(\varphi_{1k}\beta_{1k}^{-1}\beta_{2k})^2(\beta_{1k}-\varphi_{1k}), \tag{59}$$

$$\frac{1}{n}\breve{\mathbf{w}}_{1k}^{\dagger}\mathbf{g}_{2k} \xrightarrow{\text{a.s.}} -\lambda^{-1}(\varphi_{1k}\beta_{1k}^{-1}\beta_{2k})^3. \tag{60}$$

Hence, the SINR after detection satisfies

$$\begin{aligned}z_{1k} \xrightarrow{\text{a.s.}} &\varphi_{1k}\mathsf{x}_{1k} + (\varphi_{1k}\beta_{1k}^{-1}\beta_{2k})\mathsf{x}_{2k}\\ &+\lambda^{-1}(\varphi_{1k}\beta_{1k}^{-1}\beta_{2k})^2(\beta_{1k}-\varphi_{1k})\tilde{\mathsf{x}}_{1k}\\ &-\lambda^{-1}(\varphi_{1k}\beta_{1k}^{-1}\beta_{2k})^3\mathsf{x}_{2k}.\end{aligned} \tag{61}$$

The statement follows by computing the SINR of (61) and by expliciting φ_{1k} and λ in terms of ϵ and β_{lk}. □

Appendix C
Proof of Theorem 2

The below lemma is used in the proof of Theorem 2.

Lemma 2. Let $L \geqslant 2$. Denote $\bar{\boldsymbol{G}} = [\boldsymbol{g}_1, \ldots, \boldsymbol{g}_L]$, $\boldsymbol{P} = \boldsymbol{I} - (\bar{\boldsymbol{G}}\boldsymbol{c}\boldsymbol{c}^{\dagger}\bar{\boldsymbol{G}}^{\dagger})/\|\bar{\boldsymbol{G}}\boldsymbol{c}\|_2^2$ where $\boldsymbol{c}$ is a nonzero vector, and $\boldsymbol{C}_{\mathsf{y}|\mathsf{G}} = P\bar{\boldsymbol{G}}\bar{\boldsymbol{G}}^{\dagger} + \boldsymbol{I}$. Then

$$\bar{\boldsymbol{G}}^{\dagger}\left(\boldsymbol{P}\boldsymbol{C}_{\mathsf{y}|\mathsf{G}}\boldsymbol{P}^{\dagger}\right)^{+}\bar{\boldsymbol{G}} \xrightarrow{\text{a.s.}} \frac{1}{P}\left(\boldsymbol{I} - \frac{1}{\|\boldsymbol{c}\|_2^2}\boldsymbol{c}\boldsymbol{c}^{\mathsf{T}}\right). \tag{62}$$

Proof: We will use the following two properties of the Moore-Penrose pseudoinverse:

- **P1** for any unitary matrix $\boldsymbol{U}$, it results $\boldsymbol{U}^{+} = \boldsymbol{U}^{\dagger}$ and $(\boldsymbol{U}\boldsymbol{A}\boldsymbol{U}^{\dagger})^{+} = (\boldsymbol{U}^{\dagger})^{+}\boldsymbol{A}^{+}\boldsymbol{U}^{+}$;
- **P2** for any invertible diagonal matrix $\boldsymbol{\Lambda}$, it results $\boldsymbol{\Lambda}^{1/2}\boldsymbol{A}^{+}\boldsymbol{\Lambda}^{1/2} = (\boldsymbol{\Lambda}^{-1/2}\boldsymbol{A}\boldsymbol{\Lambda}^{-1/2})^{+}$.

Moreover, since $n^{-1}\bar{\boldsymbol{G}}\bar{\boldsymbol{G}}^{\dagger} \xrightarrow{\text{a.s.}} \boldsymbol{D}$ where $\boldsymbol{D}$ is a diagonal matrix with positive diagonal elements, we define $\boldsymbol{Q}_n$ such that $n^{-1/2}\bar{\boldsymbol{G}} = \boldsymbol{Q}_n\boldsymbol{D}^{1/2}$. As $n \to \infty$, $\boldsymbol{Q}_n$ becomes unitary, and $\boldsymbol{Q}_n^{\dagger}\boldsymbol{Q}_n \xrightarrow{\text{a.s.}} \boldsymbol{I}$. We will assume in the remainder of the proof that $\boldsymbol{Q}_n$ is unitary for all n: it can be a posteriori verified that the final result is valid in the limit. Using the two above mentioned properties **P1** and **P2**, and expliciting $\bar{\boldsymbol{G}}$ in terms of $\boldsymbol{Q}_n$ and $\boldsymbol{D}$ allows to rewrite the RHS of (62) as

$$\bar{\boldsymbol{G}}^{\dagger}\left(\boldsymbol{P}\boldsymbol{C}_{\mathsf{y}|\mathsf{G}}\boldsymbol{P}^{\dagger}\right)^{+}\bar{\boldsymbol{G}} = \left(\boldsymbol{D}^{-1/2}\boldsymbol{Q}_n^{\dagger}\boldsymbol{P}\frac{\boldsymbol{C}_{\mathsf{y}|\mathsf{G}}}{n}\boldsymbol{P}^{\dagger}\boldsymbol{Q}_n\boldsymbol{D}^{-1/2}\right)^{+}. \tag{63}$$

Since $\boldsymbol{Q}_n$ is unitary, it is an isometry, hence $\|\boldsymbol{Q}_n\boldsymbol{D}^{1/2}\boldsymbol{c}\|_2 = \|\boldsymbol{D}^{1/2}\boldsymbol{c}\|_2$. Denote $\alpha = 1/\|\boldsymbol{D}^{1/2}\boldsymbol{c}\|_2^2$. After straightforward computations, the argument of the pseudoinverse in the RHS of (63) simplifies in

$$\begin{aligned}\boldsymbol{D}^{-1/2}\boldsymbol{Q}_n^{\dagger}\boldsymbol{P}n^{-1}\boldsymbol{C}_{\mathsf{y}|\mathsf{G}}\boldsymbol{P}^{\dagger}\boldsymbol{Q}_n\boldsymbol{D}^{-1/2}&\\ = P\boldsymbol{I} - \alpha P\boldsymbol{c}\boldsymbol{c}^{\dagger}\boldsymbol{D} - \alpha P\boldsymbol{D}\boldsymbol{c}\boldsymbol{c}^{\dagger}&\\ + \alpha^2 P\boldsymbol{c}\boldsymbol{c}^{\dagger}\boldsymbol{D}^2\boldsymbol{c}\boldsymbol{c}^{\dagger} + \Theta(n^{-1})&\end{aligned} \tag{64}$$

where $\Theta(n^{-1})$ represents a matrix with elements that scale as n^{-1}. Once the vanishing term is discarded, it can be verified from the definition of pseudoinverse that the RHS of (62) is the pseudoinverse of (64). □

Proof of Theorem 2: Following Lemma 1, we consider an equivalent system where users $j \neq k$ are ignored since they do not asymptotically interfere. This allows to replace, in the definition of $\breve{\mathbf{w}}_{1k}$ (cf. (25)), $\breve{\mathbf{U}}_{\hat{\mathbf{G}}_1}$ with

$$\boldsymbol{\Pi}_{\hat{\mathbf{g}}_{1k}}^{\perp} = \boldsymbol{I} - \frac{1}{\|\hat{\mathbf{g}}_{1k}\|_2^2}\hat{\mathbf{g}}_{1k}\hat{\mathbf{g}}_{1k}^{\dagger} \asymp \boldsymbol{I} - \varphi_{1k}^{-1}n^{-1}\hat{\mathbf{g}}_{1k}\hat{\mathbf{g}}_{1k}^{\dagger}. \tag{65}$$

From (65), (25) is asymptotically equivalent to

$$\breve{\mathbf{w}}_{1k} \asymp -\boldsymbol{\Pi}_{\hat{\mathbf{g}}_{1k}}^{\perp}\left(\boldsymbol{\Pi}_{\hat{\mathbf{g}}_{1k}}^{\perp}\boldsymbol{C}_{\mathsf{y}|\mathsf{G}}\boldsymbol{\Pi}_{\hat{\mathbf{g}}_{1k}}^{\perp}\right)^{+}\boldsymbol{\Pi}_{\hat{\mathbf{g}}_{1k}}^{\perp}\boldsymbol{C}_{\mathsf{y}'|\mathsf{G}'}\dot{\mathbf{w}}_{1k}, \tag{66}$$

where the pseudoinverse is used in place of the inverse since $\boldsymbol{\Delta} := \boldsymbol{\Pi}_{\hat{\mathbf{g}}_{1k}}^{\perp}\boldsymbol{C}_{\mathsf{y}|\mathsf{G}}\boldsymbol{\Pi}_{\hat{\mathbf{g}}_{1k}}^{\perp}$ is not full rank. In the equivalent system,

$\dot{\mathbf{w}}_{1k}$ tends to be proportional to $\hat{\mathbf{g}}_{1k}$. Expressing the variable after detection z_{1k} in terms of the detector components $\dot{\mathbf{w}}_{1k} = \hat{\mathbf{g}}_{1k}$ and $\breve{\mathbf{w}}_{1k}$ and using (38) yields

$$z_{1k} \asymp \varphi_{1k}\mathsf{x}_{1k} + \theta_{1k}\sum_{j>1}\beta_{jk}x_{jk} + \frac{1}{n}\breve{\mathbf{w}}_{1k}^{\dagger}\mathbf{g}_{1k}\tilde{\mathsf{x}}_{1k} + \sum_{j>1}\frac{1}{n}\breve{\mathbf{w}}_{1k}^{\dagger}\mathbf{g}_{jk}x_{jk}, \quad (67)$$

where we explicited $\tilde{\mathbf{g}}_{1k} = \mathbf{g}_{1k} - \hat{\mathbf{g}}_{1k}$ and used the fact that $\breve{\mathbf{w}}_{1k}$ is asymptotically orthogonal to $\hat{\mathbf{g}}_{1k}$. We prove that the normalized projection of $\breve{\mathbf{w}}_{1k}$ onto interfering out-of-cell user channels is

$$\frac{1}{n}\breve{\mathbf{w}}_{1k}^{\dagger}\mathbf{g}_{jk} \xrightarrow{\text{a.s.}} \frac{1}{L}\theta_{1k}\Big(-L\beta_{jk}\mathbb{1}_{\{j>1\}} + \sum_{i>1}\beta_{ik}\Big). \quad (68)$$

Indeed, setting $\dot{\mathbf{w}}_{1k} = \hat{\mathbf{g}}_{1k}$ in (66) yields

$$\frac{1}{n}\breve{\mathbf{w}}_{1k}^{\dagger}\mathbf{g}_{jk} \asymp -\frac{1}{n}\hat{\mathbf{g}}_{1k}^{\dagger}\boldsymbol{C}_{\mathbf{y}'|\mathsf{G}'}\boldsymbol{\Pi}_{\hat{\mathbf{g}}_{1k}}^{\perp}\boldsymbol{\Delta}^{+}\boldsymbol{\Pi}_{\hat{\mathbf{g}}_{1k}}^{\perp}\mathbf{g}_{jk}. \quad (69)$$

Since $\boldsymbol{C}_{\mathbf{y}'|\mathsf{G}'}$ is premultiplied by a vector in $\mathrm{range}\{\hat{\mathbf{g}}_{1k}\}$ and postmultiplied by an operator that removes components in $\mathrm{range}\{\hat{\mathbf{g}}_{1k}\}$, it can be replaced by $P\sum_{l>1}\mathbf{g}_{lk}\mathbf{g}_{lk}^{\dagger}$, and (69) becomes

$$\frac{1}{n}\breve{\mathbf{w}}_{1k}^{\dagger}\mathbf{g}_{jk} \asymp -P\sum_{l>1}\theta_{1k}\beta_{lk}\mathbf{g}_{lk}^{\dagger}\boldsymbol{\Pi}_{\hat{\mathbf{g}}_{1k}}^{\perp}\boldsymbol{\Delta}^{+}\boldsymbol{\Pi}_{\hat{\mathbf{g}}_{1k}}^{\perp}\mathbf{g}_{jk}. \quad (70)$$

Observing that

$$\boldsymbol{\Pi}_{\hat{\mathbf{g}}_{1k}}^{\perp}\mathbf{g}_{jk} \asymp \mathbf{g}_{jk} - \frac{1}{\varphi_{1k}}\theta_{1k}\beta_{jk}\hat{\mathbf{g}}_{1k} = \mathbf{g}_{jk} - \beta_{1k}^{-1}\beta_{jk}\theta_{1k}\sum_{i\geqslant 1}\mathbf{g}_{ik} = \sum_{i\geqslant 1}q_{jik}\mathbf{g}_{ik}, \quad (71)$$

where $q_{jik} = \delta_{ji} - \beta_{1k}^{-1}\beta_{jk}\theta_{1k}$, (70) reduces to

$$\frac{1}{n}\breve{\mathbf{w}}_{1k}^{\dagger}\mathbf{g}_{jk} \asymp -P\sum_{l>1}\theta_{1k}\beta_{lk}\sum_{i\geqslant 1}\sum_{m\geqslant 1}q_{lik}q_{jmk}\mathbf{g}_{ik}^{\dagger}\boldsymbol{\Delta}^{+}\mathbf{g}_{mk}. \quad (72)$$

Now we use Lemma 2 with $\boldsymbol{c} = \mathbf{1}_L$, where $\mathbf{1}_L$ is an L-dimensional vector of 1's, and $\epsilon = 0$ (cf. (6)) to conclude

$$\mathbf{g}_{lk}^{\dagger}\boldsymbol{\Delta}^{+}\mathbf{g}_{mk} \xrightarrow{\text{a.s.}} \frac{1}{P}\Big(\delta_{lm} - \frac{1}{L}\Big). \quad (73)$$

Using (73) in (72) yields

$$\frac{1}{n}\breve{\mathbf{w}}_{1k}^{\dagger}\mathbf{g}_{jk} \asymp -\sum_{l>1}\theta_{1k}\beta_{lk}\sum_{i\geqslant 1}\sum_{m\geqslant 1}q_{lik}q_{jmk}\Big(\delta_{im} - \frac{1}{L}\Big) \quad (74)$$

and, therefore, (68) by expliciting q_{abc} terms. By applying (68) to the last two terms in (67), we obtain

$$\frac{1}{n}\breve{\mathbf{w}}_{1k}^{\dagger}\mathbf{g}_{1k}\tilde{\mathsf{x}}_{1k} \xrightarrow{\text{a.s.}} \frac{\theta_{1k}}{L}\sum_{i>1}\beta_{ik}\tilde{\mathsf{x}}_{1k}, \quad (75)$$

$$\frac{1}{n}\breve{\mathbf{w}}_{1k}^{\dagger}\mathbf{g}_{jk}\mathsf{x}_{jk}, \xrightarrow{\text{a.s.}} \frac{\theta_{1k}}{L}\Big(-L\beta_{jk}\mathbb{1}_{\{j>1\}} + \sum_{i>1}\beta_{ik}\Big)\mathsf{x}_{jk}, \quad (76)$$

hence (67) can be simplified to

$$z_{1k} \xrightarrow{\text{a.s.}} \varphi_{1k}\mathsf{x}_{1k} + \Big\{\frac{1}{L}\theta_{1k}\sum_{i>1}\beta_{ik}\Big\}\tilde{\mathsf{x}}_{1k} + \sum_{j>1}\Big\{\frac{1}{L}\theta_{1k}\sum_{i>1}\beta_{ik}\Big\}\mathsf{x}_{jk}. \quad (77)$$

The asymptotic SINR corresponding to the RHS in (77) is

$$\bar{\gamma}_{1k} = \frac{\varphi_{1k}^2}{\Big\{\frac{1}{L}\theta_{1k}\sum_{i>1}\beta_{ik}\Big\}^2 + \sum_{l>1}\Big\{\frac{1}{L}\theta_{1k}\sum_{i>1}\beta_{ik}\Big\}^2}, \quad (78)$$

which yields (48) by writing θ_{1k} and φ_{1k} in terms of β_{lk}. □

Appendix D
Discussion on the MMSE Achieved by the Proposed Group-Blind Detector

In this appendix we show that the SINR achieved in Theorem 2 is the maximum achievable by detectors in the class of group-blind detectors with decomposition (21). In particular, we consider $\mathbf{w}_{1k} = \dot{\mathbf{w}}_{1k} + \breve{\mathbf{w}}_{1k}$ with $\dot{\mathbf{w}}_{1k}$ given by (23) and $\breve{\mathbf{w}}_{1k}$ derived according to the following MMSE criterion (cf. (24)):

$$\mathsf{MMSE}_{1k}^{\mathsf{GB}} = \min_{\breve{\mathbf{w}}_{1k}}\mathsf{MSE}_{1k}^{\mathsf{GB}}, \quad (79)$$

$$\mathsf{MSE}_{1k}^{\mathsf{GB}} = \mathbb{E}\{\,|\mathsf{x}_{1k} - (\dot{\mathbf{w}}_{1k} + \breve{\mathbf{w}}_{1k})^{\dagger}\mathbf{y}'|^2\,\}. \quad (80)$$

Remark 5. We investigate $\mathsf{MMSE}_{1k}^{\mathsf{GB}}$ instead of the traditional MMSE as defined by $\mathsf{MMSE}_{1k} = \min_{\mathbf{w}_{1k}}\mathbb{E}\{\,|\mathsf{x}_{1k} - \mathbf{w}_{1k}^{\dagger}\mathbf{y}'|^2\,\}$ because the latter requires the side knowledge of G_1 and $\{\mathsf{G}_l\}_{l\geqslant 2}$, which is not available due to pilot contamination.

We neglect the presence of noise by assuming $\mathbf{n} = \mathbf{0}$ in (39) and show at the end of the appendix that this assumption is inconsequential. From (23), it results $\dot{\mathbf{w}}_{1k} \asymp \|\hat{\mathbf{g}}_{1k}\|_2^{-2}\hat{\mathbf{g}}_{1k} \asymp n^{-1}\varphi_{1k}^{-1}\hat{\mathbf{g}}_{1k}$, hence

$$\dot{\mathbf{w}}_{1k}^{\dagger}\mathbf{y}' \asymp \frac{1}{n\varphi_{1k}}\hat{\mathbf{g}}_{1k}^{\dagger}\mathbf{y}' \xrightarrow{\text{a.s.}} \mathsf{x}_{1k} + \sum_{l>1}\bar{\beta}_{1k}\mathsf{x}_{lk}, \quad (81)$$

where $\bar{\beta}_{lk} = \beta_{lk}/\beta_{1k}$. Introducing (81) in (80) yields

$$\mathsf{MSE}_{1k}^{\mathsf{GB}} \asymp \mathbb{E}\bigg[\bigg|-\sum_{l>1}\bar{\beta}_{lk}\mathsf{x}_{lk} - \breve{\mathbf{w}}_{1k}^{\dagger}\mathbf{y}'\bigg|^2\bigg]. \quad (82)$$

This expression relates to the SINR in (10) as follows:

$$\gamma_{1k} \xrightarrow{\text{a.s.}} \frac{P}{\mathsf{MSE}_{1k}^{\mathsf{GB}}}, \quad (83)$$

and the maximum γ_{1k} is obtained with the minimum $\mathsf{MSE}_{1k}^{\mathsf{GB}}$, that is (79). Without loss of generality, scale $\breve{\mathbf{w}}_{1k}$ as $\breve{\mathbf{w}}_{1k} \asymp (n\varphi_{1k})^{-1}\mathbf{x}_{1k}$ for some $\mathbf{x}_{1k}$ that is orthogonal to $\hat{\mathbf{g}}_{1k}$. Denote λ_{lk} the following limit: $n^{-1}\mathbf{x}_{1k}^{\dagger}\mathbf{g}_{lk} \xrightarrow{\text{a.s.}} \lambda_{lk}$. The orthogonality of $\breve{\mathbf{w}}_{1k}$ with respect to $\hat{\mathbf{g}}_{1k}$ translates into a constraint for the set of $\{\lambda_{lk}\}_{l\geqslant 1}$ as follows:

$$\breve{\mathbf{w}}_{1k}^{\dagger}\sum_{l\geqslant 1}\mathbf{g}_{lk} \xrightarrow{\text{a.s.}} 0 \iff \sum_{l\geqslant 1}\lambda_{lk} = 0. \quad (84)$$

Since $n^{-1}\mathbf{x}_{1k}^{\dagger}\tilde{\mathbf{g}}_{1k} \asymp n^{-1}\mathbf{x}_{1k}^{\dagger}(\mathbf{g}_{1k} - \hat{\mathbf{g}}_{1k}) \asymp n^{-1}\mathbf{x}_{1k}^{\dagger}\mathbf{g}_{1k}$, it follows that

$$\breve{\mathbf{w}}_{1k}^{\dagger}\mathbf{y}' \asymp \varphi_{1k}^{-1}\lambda_{1k}\tilde{\mathsf{x}}_{1k} + \varphi_{1k}^{-1}\sum_{l>1}\lambda_{lk}\mathsf{x}_{lk}. \quad (85)$$

Introducing (85) in (82) yields

$$\mathsf{MSE}_{1k}^{\mathsf{GB}} \xrightarrow{\text{a.s.}} \mathbb{E}\left[\left|\varphi_{1k}^{-1}\lambda_{1k}\tilde{\mathsf{x}}_{1k} + \sum_{l>1}(\bar{\beta}_{lk} + \varphi_{1k}^{-1}\lambda_{lk})\mathsf{x}_{lk}\right|^2\right]$$
$$= P\varphi_{1k}^{-2}\left\{\left(\sum_{l>1}\lambda_{lk}\right)^2 + \sum_{l>1}(\theta_{1k}\beta_{lk} + \lambda_{lk})^2\right\}. \quad (86)$$

The optimum set $\{\boldsymbol{v}_{lk}\}_{l=1}^{L}$ minimizes (86) with respect to $\{\lambda_{lk}\}_{l\geqslant 1}$, which are given by

$$\lambda_{lk}^{\star} = \begin{cases} \theta_{1k}\big(-\beta_{lk} + \frac{1}{L}\sum_{j>1}\beta_{jk}\big) & \text{if } 1 < l \leqslant L, \\ -\sum_{j=2}^{L}\lambda_{jk}^{\star} & \text{if } l = 1. \end{cases} \quad (87)$$

The corresponding $\mathsf{MMSE}_{1k}^{\mathsf{GB}}$ is

$$\mathsf{MMSE}_{1k} \xrightarrow{\text{a.s.}} P\beta_{1k}^{-2}\frac{1}{L}\left(\sum_{l>1}\beta_{lk}\right)^2, \quad (88)$$

where we explicited definitions of $\lambda_{lk}^{\star}$, φ_{1k} and θ_{1k} in terms of β_{lk}, $l \geqslant 1$. Introducing (88) as the minimum $\mathsf{MSE}_{1k}^{\mathsf{GB}}$ in (83) yields the maximum SINR. It coincides with the SINR derived in Theorem 2 and shows that our detector maximizes the SINR within the class of detectors satisfying (21)–(23).

We can now show that neglecting noise at the beginning of the derivation is inconsequential. Indeed, the noise contribution to the SINR is $\|\mathbf{w}_{1k}\|_2^2 \asymp \|\dot{\mathbf{w}}_{1k}\|_2^2 + \|\breve{\mathbf{w}}_{1k}\|_2^2$, because the two terms are orthogonal. Since $\|\dot{\mathbf{w}}_{1k}\|_2^2 \asymp n^{-1}\varphi_{1k}^{-1} = O(n^{-1})$, the only term to investigate is $\|\breve{\mathbf{w}}_{1k}\|_2^2$. Indeed, since $\breve{\mathbf{w}}_{1k} \in \text{range}\{\hat{\mathbf{g}}_{1k}\}^{\perp} \cap \mathcal{S}_k \subseteq \mathcal{S}_k$ and $\{\mathbf{g}_{lk}\}_{l\geqslant 1}$ is a set of vectors that are asymptotically orthogonal, it results

$$\|\breve{\mathbf{w}}_{1k}\|_2^2 \asymp \left\|\sum_{l\geqslant 1}\frac{\breve{\mathbf{w}}_{1k}^{\dagger}\mathbf{g}_{lk}}{\mathbf{g}_{lk}^{\dagger}\mathbf{g}_{lk}}\mathbf{g}_{lk}\right\|_2^2 \asymp \varphi_{1k}^{-2}\frac{1}{n}\sum_{l\geqslant 1}\frac{(\lambda_{lk}^{\star})^2}{\beta_{lk}}, \quad (89)$$

which is $O(n^{-1})$ because, with the exception of n, all other terms are constants.

Acknowledgment

The authors wish to thank Z. Liu, M. Mohammadkarimi, L. Ruan, and T. Wang for careful reading of the manuscript.

References

[1] G. C. Ferrante, G. Geraci, T. Q. S. Quek, and M. Z. Win, "Group-blind detection with very large antenna arrays in the presence of pilot contamination," in *Proc. IEEE Int. Conf. Acoust. Speech Signal Process. (ICASSP)*, 2016, pp. 3701–3705.

[2] J. G. Andrews, S. Buzzi, W. Choi, S. V. Hanly, A. Lozano, A. C. K. Soong, and J. C. Zhang, "What will 5G be?" *IEEE J. Sel. Areas Commun.*, vol. 32, no. 6, pp. 1065–1082, 2014.

[3] F. Boccardi, R. W. Heath, A. Lozano, T. L. Marzetta, and P. Popovski, "Five disruptive technology directions for 5G," *IEEE Commun. Mag.*, vol. 52, no. 2, pp. 74–80, 2014.

[4] J. Hoydis, K. Hosseini, S. ten Brink, and M. Debbah, "Making smart use of excess antennas: Massive MIMO, small cells, and TDD," *Bell Labs Tech. J.*, vol. 18, no. 2, pp. 5–21, 2013.

[5] A. Kammoun, A. Muller, E. Bjornson, and M. Debbah, "Linear precoding based on polynomial expansion: Large-scale multi-cell MIMO systems," *IEEE J. Sel. Topics Signal Process.*, vol. 8, no. 5, pp. 861–875, 2014.

[6] M. Chiani, M. Z. Win, and H. Shin, "MIMO networks: The effects of interference," *IEEE Trans. Inf. Theory*, vol. 56, no. 1, pp. 336–349, Jan. 2010.

[7] L. Lu, G. Y. Li, A. L. Swindlehurst, A. Ashikhmin, and R. Zhang, "An overview of massive MIMO: Benefits and challenges," *IEEE J. Sel. Topics Signal Process.*, vol. 8, no. 5, pp. 742–758, 2014.

[8] F. Rusek, D. Persson, B. K. Lau, E. G. Larsson, T. L. Marzetta, O. Edfors, and F. Tufvesson, "Scaling up MIMO: Opportunities and challenges with very large arrays," *IEEE Signal Process. Mag.*, vol. 30, no. 1, pp. 40–60, 2013.

[9] T. Q. S. Quek, G. de la Roche, I. Guvenc, and M. Kountouris, *Small cell networks: deployment, PHY techniques, and resource allocation*. Cambridge University Press, 2013.

[10] D. Lopez-Perez, M. Ding, H. Claussen, and A. H. Jafari, "Towards 1 Gbps/UE in cellular systems: understanding ultra-dense small cell deployments," *IEEE Commun. Surveys & Tutorials*, vol. 17, no. 4, pp. 2078–2101, 2015.

[11] T. L. Marzetta, "Noncooperative cellular wireless with unlimited numbers of base station antennas," *IEEE Trans. Wireless Commun.*, vol. 9, no. 11, pp. 3590–3600, 2010.

[12] N. Jindal and A. Lozano, "A unified treatment of optimum pilot overhead in multipath fading channels," *IEEE Trans. Commun.*, vol. 58, no. 10, pp. 2939–2948, 2010.

[13] E. Bjornson, E. G. Larsson, and M. Debbah, "Massive MIMO for maximal spectral efficiency: How many users and pilots should be allocated?" *IEEE Trans. Wireless Commun.*, vol. PP, no. 99, pp. 1–1, 2015.

[14] E. G. Larsson, O. Edfors, F. Tufvesson, and T. L. Marzetta, "Massive MIMO for next generation wireless systems," *IEEE Commun. Mag.*, vol. 52, no. 2, pp. 186–195, 2014.

[15] E. Bjornson, M. Matthaiou, and M. Debbah, "Massive MIMO with non-ideal arbitrary arrays: Hardware scaling laws and circuit-aware design," *IEEE Trans. Wireless Commun.*, vol. 14, no. 8, pp. 4353–4368, 2015.

[16] E. Bjornson, E. G. Larsson, and T. L. Marzetta, "Massive MIMO: Ten myths and one critical question," *IEEE Commun. Mag.*, 2015 [To appear]. Available as arXiv:1503.06854.

[17] T. L. Marzetta, "Massive MIMO: An introduction," *Bell Labs Technical Journal*, vol. 20, pp. 11–22, 2015.

[18] S. Payami and F. Tufvesson, "Channel measurements and analysis for very large array systems at 2.6 GHz," in *Proc. 6th European Conference on Antennas and Propagation (EuCAP)*, 2012, pp. 433–437.

[19] J. Hoydis, C. Hoek, T. Wild, and S. ten Brink, "Channel measurements for large antenna arrays," in *Proc. IEEE International Symposium on Wireless Communication Systems (ISWCS)*, 2012, pp. 811–815.

[20] J. Vieira, S. Malkowsky, K. Nieman, Z. Miers, N. Kundargi, L. Liu, I. Wong, V. Owall, O. Edfors, and F. Tufvesson, "A flexible 100-antenna testbed for massive MIMO," in *IEEE Globecom Workshops*, 2014, pp. 287–293.

[21] J. Jose, A. Ashikhmin, T. L. Marzetta, and S. Vishwanath, "Pilot contamination and precoding in multi-cell TDD systems," *IEEE Trans. Wireless Commun.*, vol. 10, no. 8, pp. 2640–2651, 2011.

[22] H. Q. Ngo, E. G. Larsson, and T. L. Marzetta, "The multicell multiuser MIMO uplink with very large antenna arrays and a finite-dimensional channel," *IEEE Trans. Commun.*, vol. 61, no. 6, pp. 2350–2361, 2013.

[23] B. Gopalakrishnan and N. Jindal, "An analysis of pilot contamination on multi-user MIMO cellular systems with many antennas," in *Proc. IEEE Int. Workshop Signal Process. Adv. in Wireless Commun. (SPAWC)*, 2011, pp. 381–385.

[24] N. Krishnan, R. Yates, and N. Mandayam, "Cellular systems with many antennas: Large system analysis under pilot contamination," in *Proc. Annu. Allerton Conf. Commun. Control Comput.*, 2012, pp. 1220–1224.

[25] J. Hoydis, S. ten Brink, and M. Debbah, "Massive MIMO in the UL/DL of cellular networks: How many antennas do we need?" *IEEE J. Sel. Areas Commun.*, vol. 31, no. 2, pp. 160–171, 2013.

[26] F. Fernandes, A. Ashikhmin, and T. L. Marzetta, "Inter-cell interference in noncooperative TDD large scale antenna systems," *IEEE J. Sel. Areas Commun.*, vol. 31, no. 2, pp. 192–201, 2013.

[27] D. Gesbert, M. Kountouris, R. W. Heath, C.-B. Chae, and T. Salzer, "Shifting the MIMO paradigm," *IEEE Signal Process. Mag.*, vol. 24, no. 5, pp. 36–46, 2007.

[28] A. Conti, M. Z. Win, and M. Chiani, "Slow adaptive M-QAM with diversity in fast fading and shadowing," *IEEE Trans. Commun.*, vol. 55, no. 5, pp. 895–905, May 2007.

[29] X. Wang and J. Wang, "Effect of imperfect channel estimation on transmit diversity in CDMA systems," *IEEE Trans. Veh. Technol.*, vol. 53, no. 5, pp. 1400–1412, Sep. 2004.

[30] W. M. Gifford, M. Z. Win, and M. Chiani, "Antenna subset diversity with non-ideal channel estimation," *IEEE Trans. Wireless Commun.*, vol. 7, no. 5, pp. 1527–1539, May 2008.

[31] L. Toni and A. Conti, "Does fast adaptive modulation always outperform slow adaptive modulation?" *IEEE Trans. Wireless Commun.*, vol. 10, no. 5, pp. 1504–1513, May 2011.

[32] L. Cao and N. C. Beaulieu, "Closed-form BER results for MRC diversity with channel estimation errors in Ricean fading channels," *IEEE Trans. Wireless Commun.*, vol. 4, no. 4, pp. 1440–1447, Jul. 2005.

[33] W. M. Gifford, A. Conti, M. Chiani, and M. Z. Win, "On the SNR penalties of ideal and non-ideal subset diversity systems," *IEEE Trans. Inf. Theory*, vol. 58, no. 6, pp. 3708–3724, Jun. 2012.

[34] V. Kristem, N. B. Mehta, and A. F. Molisch, "Optimal receive antenna selection in time-varying fading channels with practical training constraints," *IEEE Trans. Commun.*, vol. 58, no. 7, pp. 2023–2034, Jul. 2010.

[35] A. Conti, W. M. Gifford, M. Z. Win, and M. Chiani, "Optimized simple bounds for diversity systems," *IEEE Trans. Commun.*, vol. 57, no. 9, pp. 2674–2685, Sep. 2009.

[36] H. Q. Ngo and E. G. Larsson, "EVD-based channel estimation in multicell multiuser MIMO systems with very large antenna arrays," in *Proc. IEEE Int. Conf. Acoust. Speech Signal Process. (ICASSP)*, 2012, pp. 3249–3252.

[37] R. R. Muller, L. Cottatellucci, and M. Vehkapera, "Blind pilot decontamination," *IEEE J. Sel. Topics Signal Process.*, vol. 8, no. 5, pp. 773–786, 2014.

[38] R. R. Muller, M. Vehkapera, and L. Cottatellucci, "Analysis of blind pilot decontamination," in *Proc. Asilomar Conf. on Signals, Systems and Computers (ACSSC)*, 2013, pp. 1016–1020.

[39] L. Cottatellucci, R. R. Muller, and M. Vehkapera, "Analysis of pilot decontamination based on power control," in *Proc. IEEE Veh. Technol. Conf. (VTC)*, 2013, pp. 1–5.

[40] J. G. Andrews, H. Claussen, M. Dohler, S. Rangan, and M. C. Reed, "Femtocells: Past, present, and future," *IEEE J. Sel. Areas Commun.*, vol. 30, no. 3, pp. 497–508, 2012.

[41] "Multi-antenna optimization in LTE," White Paper, Nokia, 2016. [Online]. Available: http://networks.nokia.com

[42] B. M. Hochwald, D. J. Love, S. Yan, P. Fay, and J. M. Jin, "Incorporating specific absorption rate constraints into wireless signal design," *IEEE Commun. Mag.*, vol. 52, no. 9, pp. 126–133, Sept. 2014.

[43] T. D. Novlan, H. S. Dhillon, and J. G. Andrews, "Analytical modeling of uplink cellular networks," *IEEE Trans. Wireless Commun.*, vol. 12, no. 6, pp. 2669–2679, June 2013.

[44] "5G use cases and requirements," White Paper, Nokia, 2016. [Online]. Available: http://networks.nokia.com

[45] C. S. Park, Y. P. E. Wang, G. Jongren, and D. Hammarwall, "Evolution of uplink MIMO for LTE-advanced," *IEEE Commun. Mag.*, vol. 49, no. 2, pp. 112–121, Feb. 2011.

[46] H. Q. Ngo, M. Matthaiou, T. Q. Duong, and E. G. Larsson, "Uplink performance analysis of multicell MU-SIMO systems with ZF receivers," *IEEE Trans. Veh. Technol.*, vol. 62, no. 9, pp. 4471–4483, Nov. 2013.

[47] G. Miao, "Energy-efficient uplink multi-user MIMO," *IEEE Trans. Wireless Commun.*, vol. 12, no. 5, pp. 2302–2313, May 2013.

[48] Q. Zhang, S. Jin, K. K. Wong, H. Zhu, and M. Matthaiou, "Power scaling of uplink massive mimo systems with arbitrary-rank channel means," *IEEE J. Sel. Topics Signal Process.*, vol. 8, no. 5, pp. 966–981, Oct. 2014.

[49] C. Kong, C. Zhong, A. K. Papazafeiropoulos, M. Matthaiou, and Z. Zhang, "Sum-rate and power scaling of massive MIMO systems with channel aging," *IEEE Trans. Commun.*, vol. 63, no. 12, pp. 4879–4893, Dec. 2015.

[50] A. Pitarokoilis, S. K. Mohammed, and E. G. Larsson, "Uplink performance of time-reversal MRC in massive MIMO systems subject to phase noise," *IEEE Trans. Wireless Commun.*, vol. 14, no. 2, pp. 711–723, Feb. 2015.

[51] X. Wang and A. Host-Madsen, "Group-blind multiuser detection for uplink CDMA," *IEEE J. Sel. Areas Commun.*, vol. 17, no. 11, pp. 1971–1984, 1999.

[52] J. Zhang and X. Wang, "Large-system performance analysis of blind and group-blind multiuser receivers," *IEEE Trans. Inf. Theory*, vol. 48, no. 9, pp. 2507–2523, 2002.

[53] A. Host-Madsen and X. Wang, "Performance of blind and group-blind multiuser detectors," *IEEE Trans. Inf. Theory*, vol. 48, no. 7, pp. 1849–1872, Jul 2002.

[54] Z. Xu and X. Wang, "Large-sample performance of blind and group-blind multiuser detectors: a perturbation perspective," *IEEE Trans. Inf. Theory*, vol. 50, no. 10, pp. 2389–2401, 2004.

[55] 3GPP TS 36.133, "Evolved Universal Terrestrial Radio Access (E-UTRA); requirements for support of radio resource management," 2015, v.12.9.0.

[56] B. Hassibi and B. M. Hochwald, "How much training is needed in multiple-antenna wireless links?" *IEEE Trans. Inf. Theory*, vol. 49, no. 4, pp. 951–963, 2003.

[57] S. M. Kay, *Fundamentals of Statistical Signal Processing: Estimation Theory*. Upper Saddle River, NJ, USA: Prentice-Hall, Inc., 1993.

[58] M. L. Eaton, *Multivariate Statistics: A Vector Space Approach*. Beachwood, Ohio, USA: Institute of Mathematical Statistics, 2007.

[59] E. Biglieri, J. Proakis, and S. Shamai, "Fading channels: information-theoretic and communications aspects," *IEEE Trans. Inf. Theory*, vol. 44, no. 6, pp. 2619–2692, 1998.

[60] U. Madhow, "Blind adaptive interference suppression for direct-sequence CDMA," *Proc. IEEE*, vol. 86, no. 10, pp. 2049–2069, 1998.

[61] M. Cierny, H. Wang, R. Wichman, Z. Ding, and C. Wijting, "On number of almost blank subframes in heterogeneous cellular networks," *IEEE Trans. Wireless Commun.*, vol. 12, no. 10, pp. 5061–5073, 2013.

[62] D. Lopez-Perez, I. Guvenc, and X. Chu, "Mobility management challenges in 3GPP heterogeneous networks," *IEEE Commun. Mag.*, vol. 50, no. 12, pp. 70–78, 2012.

[63] E. Telatar, "Capacity of multi-antenna Gaussian channels," *Europ. Trans. Telecommun.*, vol. 10, no. 6, pp. 585–596, Nov./Dec. 1997.

[64] M. Chiani, M. Z. Win, and A. Zanella, "On the capacity of spatially correlated MIMO Rayleigh fading channels," *IEEE Trans. Inf. Theory*, vol. 49, no. 10, pp. 2363–2371, Oct. 2003.

[65] H. Shin, M. Z. Win, J. H. Lee, and M. Chiani, "On the capacity of doubly correlated MIMO channels," *IEEE Trans. Wireless Commun.*, vol. 5, no. 8, pp. 2253–2265, Aug. 2006.

[66] T. Marzetta and B. Hochwald, "Capacity of a mobile multiple-antenna communication link in Rayleigh flat fading," *IEEE Trans. Inf. Theory*, vol. 45, no. 1, pp. 139–157, 1999.

[67] H. Shin, M. Z. Win, and J. H. Lee, "Saddlepoint approximation to the outage capacity of MIMO channels," *IEEE Trans. Wireless Commun.*, vol. 5, no. 10, pp. 2679–2684, Oct. 2006.

[68] H. Shin and M. Z. Win, "Gallager's exponent for MIMO channels: A reliability-rate tradeoff," *IEEE Trans. Commun.*, vol. 57, no. 4, pp. 972–985, Apr. 2009.

[69] A. Lozano and D. Porrat, "Non-peaky signals in wideband fading channels: Achievable bit rates and optimal bandwidth," *IEEE Trans. Wireless Commun.*, vol. 11, no. 1, pp. 246–257, 2012.

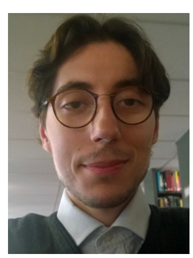

Guido Carlo Ferrante (S'11–M'15) received a double Ph.D. degree in Electrical Engineering from Sapienza Università di Roma, Rome, Italy, and CentraleSupélec, Gif-sur-Yvette, France, in April 2015. Previously, he received both M.Sc. and B.Sc. degrees (*summa cum laude*) in Electrical Engineering from Sapienza Università di Roma, Rome, Italy.

He is currently a Postdoctoral Fellow in the Wireless Information and Network Sciences Laboratory at Massachusetts Institute of Technology (MIT), Cambridge, MA, USA. Prior to joining MIT, he was a Postdoctoral Fellow at Singapore University of Technology and Design (SUTD), Singapore. His research interests include application of communication theory, information theory and statistical inference to complex systems and networks.

Dr. Ferrante received the Italian National Telecommunications and Information Theory Group Award for Ph.D. Theses in the field of Communication Technologies (2015) and the SUTD-MIT Postdoctoral Fellowship (2015–2017). He has organized a special session on 'Beyond 5G' at the 2016 Tyrrhenian International Workshop in Digital Communications, Livorno, Italy.

Giovanni Geraci (S'11–M'14) was born in Sicily, Italy. He received the B.Sc. degree in telecommunications engineering from Università degli Studi di Palermo, Palermo, Italy, in 2005, and the M.Sc. degree in Telecommunications Engineering from Politecnico di Milano, Milano, Italy, in 2009, and the Ph.D. degree in Electrical Engineering from the University of New South Wales (UNSW), Sydney, NSW, Australia, in 2014.

He is currently a Member of Technical Staff at Bell Labs Nokia, Ireland. Prior to joining Bell Labs, he was a Postdoctoral Fellow with the Singapore University of Technology and Design (SUTD), Singapore. He has also held internships at Supélec, Gif-sur-Yvette, France, and at the University of Texas at Austin, USA. His research interests cover various aspects of wireless communications, networking, and signal processing.

Tony Q.S. Quek (S'98-M'08-SM'12) received the B.E. and M.E. degrees in Electrical and Electronics Engineering from Tokyo Institute of Technology, Tokyo, Japan, respectively, and the Ph.D. in Electrical Engineering and Computer Science from Massachusetts Institute of Technology (MIT), Cambridge, MA, USA. He is currently a tenured Associate Professor with the Singapore University of Technology and Design (SUTD). He also serves as the deputy director of the SUTD-ZJU IDEA. His main research interests are the application of mathematical, optimization, and statistical theories to communication, networking, signal processing, and resource allocation problems. Specific current research topics include heterogeneous networks, green communications, wireless security, internet-of-things, big data processing, and cognitive radio.

Dr. Quek has been actively involved in organizing and chairing sessions, and has served as a member of the Technical Program Committee as well as symposium chairs in a number of international conferences. He is serving as the Workshop Chair for IEEE Globecom in 2017 and the Special Session Chair for IEEE SPAWC in 2017. He is currently an Editor for the IEEE TRANSACTIONS ON COMMUNICATIONS and an Executive Editorial Committee Member for the IEEE TRANSACTIONS ON WIRELESS COMMUNICATIONS. He was Editor for the IEEE WIRELESS COMMUNICATIONS LETTERS, Guest Editor for the IEEE SIGNAL PROCESSING MAGAZINE (Special Issue on Signal Processing for the 5G Revolution) in 2014, and the IEEE WIRELESS COMMUNICATIONS MAGAZINE (Special Issue on Heterogeneous Cloud Radio Access Networks) in 2015. He is a co-author of the book *Small Cell Networks: Deployment, PHY Techniques, and Resource Allocation* published by Cambridge University Press in 2013 and the book *Cloud Radio Access Networks: Principles, Technologies, and Applications* by Cambridge University Press.

Dr. Quek was honored with the 2008 Philip Yeo Prize for Outstanding Achievement in Research, the IEEE Globecom 2010 Best Paper Award, the 2012 IEEE William R. Bennett Prize, the IEEE SPAWC 2013 Best Student Paper Award, the IEEE WCSP 2014 Best Paper Award, the IEEE PES General Meeting 2015 Best Paper, and the 2015 SUTD Outstanding Education Awards—Excellence in Research.

Moe Z. Win (S'85-M'87-SM'97-F'04) received both the Ph.D. in Electrical Engineering and the M.S. in Applied Mathematics as a Presidential Fellow at the University of Southern California (USC) in 1998. He received the M.S. in Electrical Engineering from USC in 1989 and the B.S. (*magna cum laude*) in Electrical Engineering from Texas A&M University in 1987.

He is a Professor at the Massachusetts Institute of Technology (MIT) and the founding director of the Wireless Communication and Network Sciences Laboratory. Prior to joining MIT, he was with AT&T Research Laboratories for five years and with the Jet Propulsion Laboratory for seven years. His research encompasses fundamental theories, algorithm design, and experimentation for a broad range of real-world problems. His current research topics include network localization and navigation, network interference exploitation, intrinsic wireless secrecy, adaptive diversity techniques, and ultra-wideband systems.

Professor Win is an elected Fellow of the AAAS, the IEEE, and the IET, and was an IEEE Distinguished Lecturer. He was honored with two IEEE Technical Field Awards: the IEEE Kiyo Tomiyasu Award (2011) and the IEEE Eric E. Sumner Award (2006, jointly with R. A. Scholtz). Together with students and colleagues, his papers have received numerous awards, including the IEEE Communications Society's Stephen O. Rice Prize (2012), the IEEE Aerospace and Electronic Systems Society's M. Barry Carlton Award (2011), the IEEE Communications Society's Guglielmo Marconi Prize Paper Award (2008), and the IEEE Antennas and Propagation Society's Sergei A. Schelkunoff Transactions Prize Paper Award (2003). Highlights of his international scholarly initiatives are the Copernicus Fellowship (2011), the Royal Academy of Engineering Distinguished Visiting Fellowship (2009), and the Fulbright Fellowship (2004). Other recognitions include the IEEE Communications Society Edwin H. Armstrong Achievement Award (2016), the International Prize for Communications Cristoforo Colombo (2013), the *Laurea Honoris Causa* from the University of Ferrara (2008), the Technical Recognition Award of the IEEE ComSoc Radio Communications Committee (2008), and the U.S. Presidential Early Career Award for Scientists and Engineers (2004).

Dr. Win was an elected Member-at-Large on the IEEE Communications Society Board of Governors (2011–2013). He was the Chair (2004–2006) and Secretary (2002–2004) for the Radio Communications Committee of the IEEE Communications Society. Over the last decade, he has organized and chaired numerous international conferences. He is currently serving on the SIAM Diversity Advisory Committee, and the advisory board of the IEEE COMMUNICATION LETTERS. He served as Editor-at-Large (2012–2015) for the IEEE WIRELESS COMMUNICATIONS LETTERS, as Editor (2006–2012) for the IEEE TRANSACTIONS ON WIRELESS COMMUNICATIONS, and as Area Editor (2003–2006) and Editor (1998–2006) for the IEEE TRANSACTIONS ON COMMUNICATIONS. He was Guest-Editor for the PROCEEDINGS OF THE IEEE (2009) and for the IEEE JOURNAL ON SELECTED AREAS IN COMMUNICATIONS (2002).